coatings

MDPI

Review

Surface Modifications of Magnesium-Based Materials for Hydrogen Storage and Nickel–Metal Hydride Batteries: A Review

Yinglong Kang [1], Kemin Zhang [1,*] and Xi Lin [2,3,*]

[1] School of Materials Science and Engineering, Shanghai University of Engineering Science, Shanghai 201620, China
[2] National Engineering Research Center of Light Alloys Net Forming & School of Materials Science and Engineering, Shanghai Jiao Tong University, Shanghai 200240, China
[3] Shanghai Key Laboratory of Hydrogen Science & Center of Hydrogen Science, Shanghai Jiao Tong University, Shanghai 200240, China
* Correspondence: zhangkm@sues.edu.cn (K.Z.); lxlh1992@sjtu.edu.cn (X.L.)

Abstract: Whether it is fossil energy or renewable energy, the storage, efficient use, and multi-application of energy largely depend on the research and preparation of high-performance materials. The research and development of energy storage materials with a high capacity, long cycle life, high safety, and high cleanability will improve the properties of energy storage systems and promote their wide application. In recent years, Mg-based materials, from a comprehensive consideration of energy storage performance, raw material reserves, and prices, have demonstrated potential industrial applications as large-scale hydrogen storage materials. Nevertheless, Mg-based materials also have obvious disadvantages: as a hydrogen storage material, the hydrogen absorption/desorption rate is insufficient, as well as the high hydrogen absorption/desorption temperatures; as the electrode material of Ni-MH batteries, the reactions of Mg with alkaline electrolyte and corrosion are the main problems for applications. This article reviews different surface treatment methods and mechanisms for surface modifications of Mg-based materials for hydrogen storage and Ni-MH battery applications, as well as the performance of the materials after surface modifications. Multiple experimental studies have shown that the surface layer or state of Mg-based materials has a strong impact on their performance. Surface modification treatment can greatly improve the energy storage performance of magnesium-based materials for hydrogen storage and Ni-MH battery applications. Specifically, Mg-based materials can have a lower hydrogen absorption/desorption temperature and a faster hydrogen absorption/desorption rate when used as hydrogen storage materials and can improve the corrosion resistance, initial discharge capacity, and cycling stability in alkaline solutions when used as negative electrode materials for Ni-MH batteries. By offering an overview of the surface modification methods for Mg-based materials in two energy storage fields, this article can improve researchers' understanding of the surface modification mechanism of Mg-based materials and contribute to improving material properties in a more targeted manner. While improving the material properties, the material's preparation and surface modification treatment process are considered comprehensively to promote the development, production, and application of high-performance Mg-based materials.

Keywords: energy storage; magnesium-based materials; hydrogen storage; nickel–metal hydride battery electrode materials; surface modification

check for updates

Citation: Kang, Y.; Zhang, K.; Lin, X. Surface Modifications of Magnesium-Based Materials for Hydrogen Storage and Nickel–Metal Hydride Batteries: A Review. *Coatings* **2023**, *13*, 1100. https:// doi.org/10.3390/coatings13061100

Academic Editor: Frederic Sanchette

Received: 29 May 2023
Revised: 11 June 2023
Accepted: 12 June 2023
Published: 14 June 2023

Copyright: © 2023 by the authors. Licensee MDPI, Basel, Switzerland. This article is an open access article distributed under the terms and conditions of the Creative Commons Attribution (CC BY) license (https://creativecommons.org/licenses/by/4.0/).

1. Introduction

Energy is one of the most critical material resources for the development of human society. In recent decades, rapid population growth and heavy industry development have led to a significant increase in demand for energy. The traditional energy structure dominated by fossil fuels is no longer sufficient to support the sustainable development of

human society. Therefore, one of the biggest challenges for today's society is the search for sustainable, low-cost, clean energy sources. Furthermore, it is essential to achieve higher energy efficiency while gradually adapting new energy systems. In the future, all energy systems must use traditional energy more efficiently and gradually increase the use of renewable energy sources. Although natural resources such as solar, wind, geothermal, and tidal energy are renewable, their dependence on the environment and time zones leads to shortcomings, such as intermittency, an unstable capacity, and unpredictability [1–4]. As the cleanest energy source, hydrogen energy is expected to transform the main carbon-based economy of modern society into a less- or even zero-carbon-based economy [5,6]. However, as the lightest gaseous energy source, safe and efficient storage and transportation also limit the speed of the development and broad application of hydrogen energy [7–9]. However, for the realization of energy structure adjustment and the efficient use of renewable energy, the problem of how to store energy safely and efficiently must be addressed and solved.

Energy storage is an essential intermediate link to achieving multi-purpose, easy-to-manage, and the efficient use of energy. At present, common energy storage systems include thermal, mechanical, electromagnetic, hydrogen, and electrochemical energy storage systems [10–12]. Hydrogen and electrochemical energy storage have attracted increasing research interest and widespread attention in recent years, as they are compared to traditional energy storage methods. The ability of an energy storage technology to achieve large-scale applications in modern industry and real life is also closely related to the research and development of relevant materials [13,14]. Energy storage materials play a key role in the efficient and multifunctional application of energy and are of crucial importance for the development, storage, and utilization of clean energy, as well as the construction of energy infrastructure. There are many kinds of energy storage materials that are widely used in industries. In addition, the safety of energy storage is mainly related to the environment and the choice of energy storage materials. Due to its high storage capacity, cheap price, and abundant reserves, Mg-based materials are considered one of the key types of energy storage materials with great potential applications [15–17].

Nowadays, the research of Mg-based materials for energy storage applications mainly focuses on two areas: (1) as a storage medium for hydrogen in solid-state hydrogen storage tanks and (2) as an electrode material for Ni-MH batteries. However, both of these applications suffer from certain shortcomings. The former has a high thermodynamic stability resulting in high operation temperatures and poor kinetic performances, which severely limits the development and widespread use of Mg-based hydrogen storage materials [18,19]. In the case of Ni-MH batteries, the performance largely depends on the rate of charge transfer on the electrode surface, which also includes the transfer rate of hydrogen between adsorbed and adsorbate states, as well as the diffusion of hydrogen in the adsorbed state between the interior of the material and the electrode surface [20–22]. Moreover, the alkaline electrolyte in Ni-MH batteries also causes interfacial reactions with the electrode material, accelerating the corrosion of the electrode and, thus, affecting the electrochemical performance of the battery [23,24]. Thus, the poor cycling stability performance and corrosion resistance of Mg-based materials are the obstacles for their application in Ni-MH batteries [25–28]. More and more research results show that the performance of Mg-based materials, either as hydrogen storage media or electrode materials, is closely related to the surface structure and surface state. [29–32].

On the one hand, as a hydrogen storage material, the surface layer of Mg-based materials dramatically impacts performance. It directly affects the physical and chemical adsorption and the decomposition of H_2 on the material surface, as well as the surface permeation rate of H. These factors ultimately affect the kinetic performance of hydrogen adsorption and desorption. The hydrogen absorption reaction process of materials can be described as follows (Figure 1) [33]: step 1: H_2 is physically adsorbed on the surface of particles by van der Waals forces; step 2: H_2 is chemisorbed and dissociated to H on the surface of particles; step 3: H penetrates the lattice through the surface and diffuses to the interior of the alloy; step 4: the alloy phase transforms to the hydride phase. The

hydrogen desorption reaction can be considered the reverse process of the hydrogen absorption reaction [34]. The dissociation energy barrier of H_2 on the Mg surface is as high as 218 kJ mol^{-1} H_2 [35]. The slow surface permeation rate of H on the material surface is also a key factor affecting the hydrogen absorption reaction kinetics of Mg-based materials. As is known, Mg-based materials are extremely prone to oxidation during the preparation process. The oxide layer formed on the surface hinders the decomposition of H_2 and the surface permeation of H, leading to a significant decrease in the hydrogen absorption/desorption rate [36]. Moreover, prolonged hydrogen absorption/desorption can also lead to the pulverization of the particles and the poisoning of impurity gas, which reduces the hydrogen storage capacity of the material and shortens its service life. Thus, in order to enhance the hydrogen absorption kinetics, it is necessary to increase the rate of decomposition of H_2 on the material surface, the permeation rate of H on the surface, and the ability of the surface to resist impurity gas poisoning. However, these all directly depend on the composition, structure, and state of the material surface.

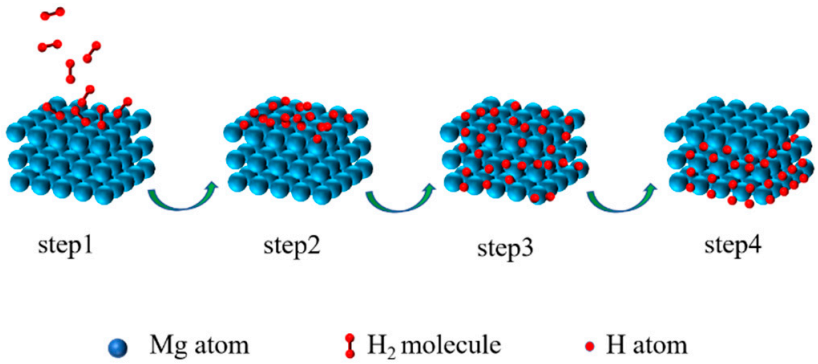


Figure 1. Schematic illustration of the hydrogen absorption process of Mg.

On the other hand, when Mg-based materials are prepared as electrodes for Ni-MH batteries, the main processes that occur at the electrodes during charging are the decomposition of water into H at the material's surface and the diffusion of H to the surface and inside the material. When the counter-current is applied, H is released and oxidized to water [37,38]. Two main factors dictate the electrochemical kinetic performance of electrodes: the ability of hydrogen diffusion inside the material and the ability of charge transfer on the surface of the material [39,40]. Furthermore, electrons are conducted to the electrolyte through the propagation medium of the material surface, so a key factor influencing the electrode reaction is a surface with good electron conductivity. In addition, the surface of the electrode material is also highly susceptible to corrosion in alkaline electrolytes. As a result, the material surface's ability to resist corrosion also plays a crucial role in determining the electrode's cycling stability and service life.

2. Surface Modification of Magnesium-Based Materials

The properties of Mg-based materials are closely related to their composition, crystal structure, and surface state. Generally, thermodynamic properties, such as the maximum capacity and enthalpy change, are directly related to the material composition and crystal structure [41]. However, the surface state significantly impacts the kinetics [42], as well as the properties of surface corrosion resistance, impurity toxicity resistance, and electrocatalytic activity. These factors, in turn, affect the overall performance of the material. To improve the performance of Mg-based materials, various surface modification techniques, such as surface coatings, surface catalysis, nanocrystallization and amorphization, and the formation of core–shell structures, are often employed. These techniques have supported the application of Mg-based materials in fields such as hydrogen storage and Ni-MH batteries.

2.1. Surface Modifications of Hydrogen Storage Material

In recent years, an important research direction for Mg-based materials is their application as a hydrogen storage and transportation medium. In this field, the hydrogen absorption/desorption rate, temperature, and storage capacity are the primary concerns. From a kinetic perspective, the main reasons for the slow hydrogen absorption reaction of Mg-based materials include the following: (1) the MgO or $Mg(OH)_2$ layer on the material's surface inhibits the decomposition of H_2 and the penetration and diffusion of H on the surface [43], and (2) after the initial production of MgH_2 on the surface, the subsequent diffusion of H gradually becomes more difficult [44–46]. Therefore, it is essential to accelerate H_2 decomposition and H diffusion on the material surface to improve the hydrogen absorption/desorption rate. Surface modification techniques, such as surface catalytic treatment, nanocrystalline treatment, and the formation of core–shell structures, are crucial for enhancing the surface performance of Mg-based materials.

2.1.1. Surface Catalytic Treatment

One of the commonly used methods to improve the hydrogen storage property of Mg-based materials is to add a catalytic phase to their surface. Such an addition can create more active sites and channels for H_2 decomposition and H diffusion, thereby significantly improving the hydrogen absorption/desorption rate of materials [47–50]. Transition metals and their oxides are currently the most extensively studied catalysts. These catalysts can accelerate H_2 decomposition on the surface of Mg-based materials, thereby improving the kinetic properties of materials at lower temperatures [51,52].

Nanoscale transition metal clusters can further enhance the catalytic effect of transition metals. However, both the clusters and Mg particles are susceptible to aggregation, which negatively impacts the hydrogen absorption/desorption rate [53]. Mesoporous and microporous materials can be used as dispersed phases to separate the nanoclusters to prevent them from aggregation [54–56]. Numerous studies have investigated the use of carbon materials as a dispersed phase to prevent the aggregation of nano-transition metal clusters and improve the properties of Mg-based materials [57–60]. Liu et al. [61] prepared Ni@rGO nanomaterials with porous structures using reduced graphene oxide (rGO) as a carrier loaded with the nano-transition metal Ni, and then they synthesized a MgH_2-5 wt% Ni@rGO composite material via ball milling. It was found that the composite material had a faster desorption rate and a lower desorption temperature than the untreated MgH_2 material, which all stemmed from the distribution of Ni@rGO nanoparticles on the surface of the MgH_2 particles. A small amount of laminated rGO flakes was also found on the surface of MgH_2. Furthermore, these flakes prevented the sintering and agglomeration of nanoparticles, accelerating the decomposition of MgH_2 and enhancing the cycling stability. Liu et al. [62] synthesized Co with a uniform size of 10 nm and loaded it on carbon nanotubes to form Co@CNT materials, which were then doped into MgH_2 to form MgH_2/Co@CNT composites. This material can desorb H_2 rapidly at 267.8 °C and desorb 6.89 wt% H_2 at 300 °C within 15 min. By performing XRD, TEM, and EDS characterizations on the MgH_2/Co@CNT composites, it was discovered that Co@CNTs exhibit a good catalytic effect on the hydrogen absorption/desorption reaction of materials. The phase transition from Mg_2Co to Mg_2CoH_5 on Co@CNTs can improve the hydrogen absorption/desorption process by creating a "hydrogen channel" effect. Additionally, carbon nanotubes are elongated into carbon sheets and uniformly cover the surface of MgH_2 particles. This carbon nanotube coverage on the MgH_2 particles has a synergistic effect (Figure 2), which reduces the hydrogen absorption/desorption temperature and further enhances the kinetics of MgH_2.

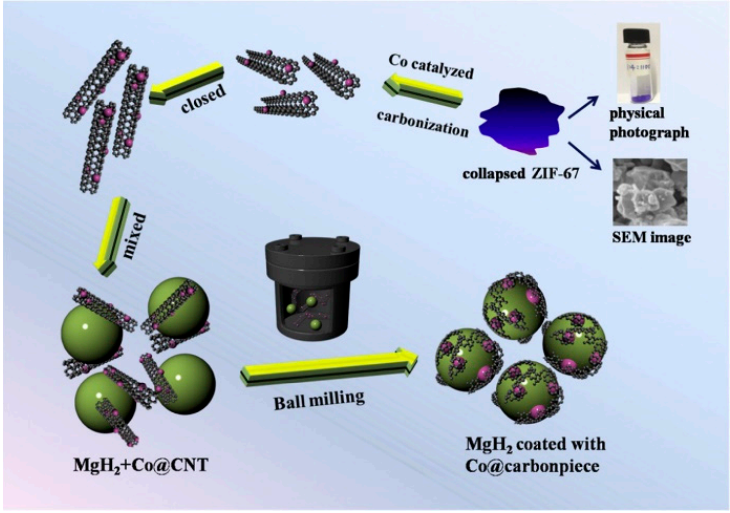


Figure 2. Schematic illustration of MgH_2/Co@CNT and its synergetic catalytic effect. Reprinted with permission from Ref. [62]. Copyright 2019, Elsevier.

Hudson et al. [63] investigated and improved the kinetics of Mg-based materials by synthesizing graphene-containing iron nanoclusters. It was found that this graphene could accelerate the hydrogen desorption process. The graphene structure creates more active sites for hydrogen desorption, and the presence of iron nanoclusters reduces the adsorption of H during hydrogen desorption, thus allowing for low-temperature hydrogen desorption.

Bhatnagar et al. [64] synthesized catalytic Fe_3O_4@GS composites using Fe_3O_4 nanoparticles and graphene sheets (GSs) and experimentally verified that such composites can improve the kinetics and thermodynamics of the performance of Mg-based hydrogen storage materials. Fe_3O_4@GS exhibited a superior catalytic effect during hydrogen desorption compared to GS or Fe_3O_4, with a lower onset hydrogen desorption temperature (262 °C) and desorption activation energy (90.53 kJ mol^{-1} H_2), leading to an improvement in the hydrogen absorption rate and storage capacity. The enhancement of catalytic activity was mainly due to the synergistic effect of iron nanoparticles and GS. GS ensures a homogeneous dispersion of the Fe nanoparticles, preventing their agglomeration, increasing the effective surface area for catalysis, and improving the catalyst's durability and stability. Furthermore, the variable valence of Fe enables GS to function as an intermediate carrier, accelerating charge transfer during the hydrogen absorption/desorption process (Figure 3).

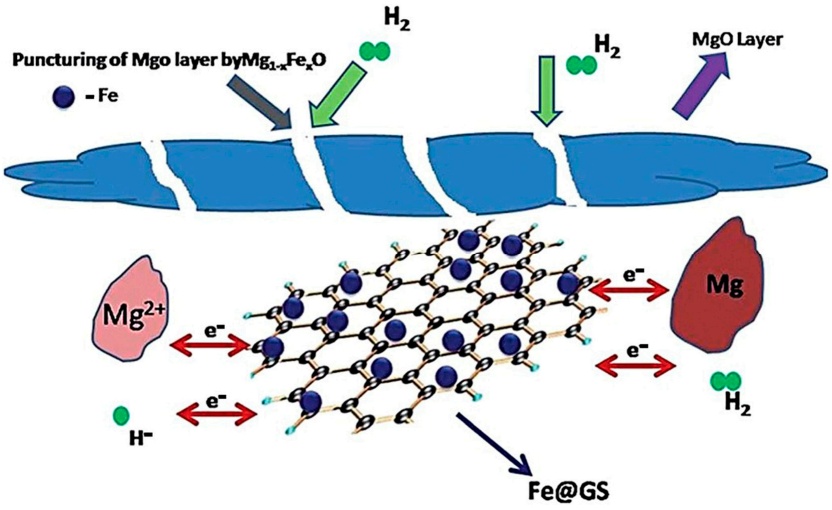


Figure 3. Schematic representation of catalytic mechanism of Fe_3O_4@GS on MgH_2/Mg. Reprinted with permission from Ref. [64]. Copyright 2016, Royal Society of Chemistry.

Xie et al. [65] prepared Mg-5 wt%NiS/rGO nanocomposites using reduced graphene oxide (rGO) modified with nickel sulfide and nano-Mg powder as raw materials through hybrid ball milling. The composites exhibited excellent hydrogen desorption kinetics, rapidly desorbing 3.7 wt% of H_2 in 10 min and 4.5 wt% of H_2 in 60 min. It was found that 800 nm of nickel sulfides was completely transformed into catalysts such as MgS, Mg_2Ni, and Ni after the first hydrogenation of the material. The excellent hydrogen desorption performance was derived from the highly dispersive catalysts, such as MgS, Mg_2Ni, and Ni, which had a synergistic catalytic effect on the rGO flakes (Figure 4), and the formation of more nucleation sites between rGO flakes, catalysts, and the Mg matrix.

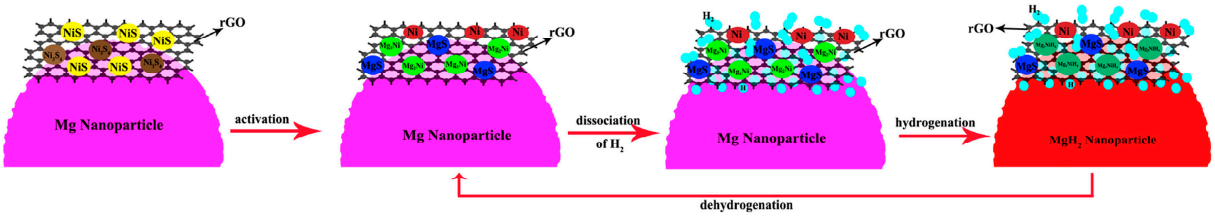


Figure 4. Schematic illustration of the catalytic mechanism of Ni, Mg_2Ni, MgS, and rGO during the hydrogen absorption/desorption processes of the Mg-NiS/rGO nanocomposite. Reprinted with permission from Ref. [65]. Copyright 2017, Elsevier.

Wang et al. [66] developed a composite catalyst that allows for the homogeneous dispersion of ultrafine Ni nanoparticles on porous carbon nanospheres. Ni nanoparticles have a high activity and can form nanosized Mg_2Ni/Mg_2NiH_4, which acts as the catalyst in the reaction process. At the same time, carbon groups can also make the catalyst highly dispersed to obtain sustainable catalytic activity. Ma et al. [67] treated 5 wt% TiH_2, 2 wt% graphite, and a mixture of the two as additives with Mg_2NiH_4 for ball milling. After air exposure, the kinetic properties of the materials were improved, especially with the composites incorporating both TiH_2 and graphite. The exceptional air stability and kinetics of the Mg_2NiH_4-TiH_2 composites can be attributed to three synergistic effects, including the protection of the passivation layer, the catalytic of TiH_2, and the catalytic of the Ni-based products formed in situ in the composite. This synergistic effect prevents further oxidation of the material surface and provides more active sites for the hydrogen absorption/desorption reaction. Moreover, the discovery of this synergistic effect can provide guidance for the study and development of Mg-based materials with both excellent air stability and high activity.

When it comes to modifying surfaces with catalysts, transition metals are typically the preferred choice. In order to enhance the efficiency of this process, researchers have focused on reducing the catalysts' particle size to the nanoscale and incorporating carbon materials with porous structures to prevent particle agglomeration. Comprehensive studies have shown that transition metals and their alloys exhibit excellent catalytic properties in the process of the hydrogen absorption/desorption of Mg-based materials and can significantly decrease the temperature of the hydrogen absorption/desorption of the materials. In particular, the combination of carbon materials and nanocatalytic particles, the porous structure of carbon materials, and the size effect of nano-transition metal particles contribute to the maintenance and enhancement of surface catalyst catalysis. However, the search for catalysts that can maintain the good hydrogen storage capacity and cycling stability of the material remains a challenge.

2.1.2. Nanocrystallization Treatment

By utilizing unique preparation methods to reduce the particle size to the nanoscale, surface energy is significantly enhanced, and lattice defects are increased, resulting in a considerable improvement in the hydrogen absorption/desorption performance of materials [68–70]. Nanosizing has been extensively studied as a modification technique for Mg-based materials since the end of the last century and has been shown to enhance

this material's hydrogen storage capabilities significantly. Currently, the preparation processes of nano Mg-based materials mainly involve mechanical grinding, gas-phase, and nano-confinement processes.

Zaluski [71] and Zaluska [18] firstly discovered and demonstrated that ball milling could improve the properties of MgH_2. Mechanical grinding is an effective method for preparing highly reactive Mg-based materials on the nanoscale while also introducing porous surface structures, internal structure defects, and surface microstrain. These alterations ultimately reduce the energy needed for H_2 to decompose on the material surface, promote the diffusion of H within the material, and enhance the kinetic properties of the material [72,73].

Zhang et al. [74] utilized mechanical grinding to prepare $La_7Sm_3Mg_{80}Ni_{10}$ + 5 wt% TiO_2 composites, with a focus on the impact of ball milling time (5–20 h) on the structure and hydrogen absorption/desorption kinetics. The findings indicate that the composites exhibit optimal activation and kinetic properties after 10 h of ball milling. Ball milling leads to the gradual transformation of material structures into nanocrystalline and amorphous, which results in a lowered activation energy. Moreover, an increase in ball milling time also leads to an increase in alloy crystal defects and a change in the surface state, which makes H_2 adsorption on the material particle surface easier, and H has shorter and more diffusion paths, allowing the material to absorb hydrogen faster. The ability of nanosizing treatment to enhance the hydrogen absorption performance of materials has also long been demonstrated, with the surface hydrogen absorption capacity of nanocrystalline particles being much higher than that of coarse polycrystalline particles [39]. Chen et al. [75] synthesized the ternary nano-metallic hydride material Mg_2CoH_5 via mechanical grinding under a hydrogen atmosphere. The sample had nanocrystalline structural features, a high specific surface area, and good hydrogen absorption kinetic properties. Herrich et al. [76] also synthesized nanoscale Mg_2FeH_6 composites via mechanical grinding. Material powders with a particle size of less than 20 nm can store 5.2 wt% of H_2. Meanwhile, iron can act as a catalyst during the hydrogen desorption process, thus reducing the hydrogen desorption temperature of Mg_2FeH_6 powder.

Li et al. [77] prepared Mg nanowires with diameters in the range of 30–170 nm by using a vapor transport method. Compared with the bulk Mg/MgH_2 material, the Mg nanowires possess better kinetic properties for hydrogen absorption/desorption. It is also predicted that if the diameter of the nanowires is less than 30 nm, further changes in the kinetics and thermodynamics of the materials will occur. Venturi et al. [78] prepared Mg nanoparticles with an initial size of 10–50 nm by using inert gas condensation and deposited them onto the substrate material at room temperature. During the deposition process, magnesium nanoparticles coarsen significantly. Both the degree of coarsening and the final morphology are related to the anisotropy of the surface energy of the material. This finding has great significance for the synthesis and stability of the nanostructures of Mg or other elements with similar characteristics.

Choi et al. [79] synthesized Mg-5%Ti nanomaterials through chemical vapor synthesis (CVS) and examined the hydrogen storage performance of the materials. The tests revealed that the initial hydrogen discharge temperature of the Mg-Ti nanomaterials (381 °C) was much lower than that of pristine MgH_2. In addition, the hydrogen desorption activation energy of the material was reduced to 104 kJ mol^{-1} (153 kJ mol^{-1} for MgH_2). This experiment shows that Mg-based materials with low agglomeration can be synthesized by using the gas-phase method, which dramatically improves the kinetic performance of the materials in the hydrogen desorption process. Nano-confinement is a method that involves the loading of hydrogen storage materials into nanoporous materials to enhance their thermodynamic and kinetic properties [80,81]. There are two main aspects to this approach: firstly, decreasing the particle size to the nanoscale and then loading them into pores and, secondly, ensuring the stability of the resulting nanostructure of the material. Porous carbon and organic matter have a high specific surface area, multi-scale pore size

distribution, and excellent stability, and they are currently the main porous materials used in the nano-confinement of Mg-based materials.

Zlotea et al. [82] reported a solid hydrogen storage material synthesized from Mg-based nanoparticles and mesoporous carbon. The pore of mesoporous carbon can act as the reactor of nanoparticles, which prevents the nanoparticles from condensing into larger aggregates and greatly enhances the hydrogen desorption kinetics of the material. Zhang et al. [83] used a dibutyl magnesium ($MgBu_2$) precursor solution to permeabilize carbon aerogels (pore size 13 nm), followed by the hydrogenation of $MgBu_2$ precursors at a 5–6 MPa pressure and 170 °C. The material characterization showed that the MgH_2 obtained after the treatment was confined in the aerogel pores as nanoparticles, and the hydrogen desorption rate was five times faster than that of the ball-milled MgH_2. Confining metal hydrides in the nanoporous scaffold can avoid the aggregation of hydride particles during the cycling process, enhancing the hydrogen desorption kinetic performance of the material. Zlotea et al. [84] reported a solid hydrogen storage material synthesized from Mg-based nanoparticles and mesoporous carbon. The pore of mesoporous carbon can act as the reactor for nanoparticles, which prevents the nanoparticles from coarsening into larger aggregates and extremely improves the hydrogen desorption kinetics of the material. Chen et al. [85] used reactive gas evaporation to confine Mg nanoparticles decorated with V in a 1 nm carbon shell, and the hydrogen storage performances of the material were greatly improved. An analysis indicated that the enhanced performance was primarily attributed to the carbon shell's nano-confinement effect and the VH_2/V_2H nanoparticles' catalytic effect as a "hydrogen pump" during the process of the reaction. Jia et al. [86] suggested a technique for incorporating nanoscale MgH_2 into ordered mesoporous carbon materials that introduced size effects and scaffold interface nano-constraints, resulting in hydrogen desorption at lower temperatures (50 °C) in comparison to the use of carbon aerogel. Theoretical calculations were conducted, proposing a potential facilitation mechanism for interfacial bonding between Mg nanoparticles and unsaturated carbon, which leads to the transfer of electrons from MgH_2 to the carbon support, ultimately weakening the Mg-H bond.

Furthermore, researchers have found that the chemical interactions on the surface of functional nanoparticles during hydrogen absorption are strongly linked to the crystal facets of the material. Therefore, there is promising potential for synthesizing nanomaterials with a selective orientation based on this discovery [87,88]. Combined with the fact that rGO can limit the particle size of Mg, Dun et al. [89] grew Mg nanoparticles with preferential orientation on reduced graphene oxide (rGO). Experiments and first-principles calculations consistently show that materials with preferentially oriented crystal surfaces have better hydrogen absorption properties. Although the research in this area is still lacking, the combination of experiments and simulations also lays the foundation for the study of hydrogen storage materials with preferentially oriented crystal surfaces.

Numerous theoretical and experimental studies have reported that the thermodynamic performance of the Mg/MgH_2 system can be significantly improved through the size effect of the material particles when the Mg/MgH_2 particle size decreases to 3 nm [90,91]. On this basis, researchers have analyzed the effect of grain size on the hydrogen desorption performance and thermodynamic stability of Mg/MgH_2 with the help of quantum mechanical calculations. The results show that nanostructured MgH_2 clusters have a lower desorption enthalpy than bulk MgH_2. The effect of the variation in the grain size on the total energy of MgH_2 and the degree of binding of Mg nanoparticles to H_2 molecules can be given (Figure 5) [92]. It has been observed that, when the particle size is less than 1.5 nm, the total energy of the MgH_2 group becomes smaller, and such a reduction can improve the thermodynamic properties of the materials to a great extent. However, it has also been shown that, even when nanoparticles have larger sizes, the thermodynamic properties of the material change considerably (Figure 6) [93]. Furthermore, as nanoparticles with larger dimensions are easier to prepare and handle, this opens a new perspective for using particle size effects to enhance the hydrogen storage performance of Mg-based materials.

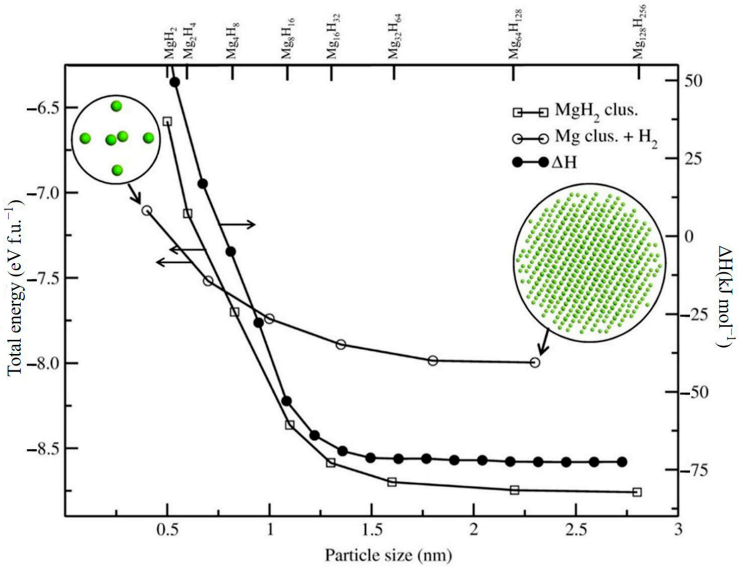


Figure 5. Effect of size on the total energy of MgH_2 nanoparticles. Reprinted with permission from Ref. [92]. Copyright 2012, American Chemical Society.

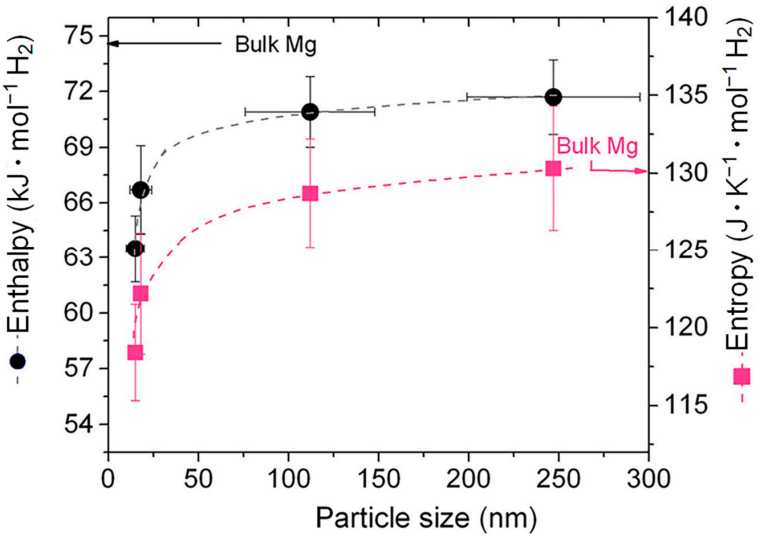


Figure 6. Changes in ΔH and ΔS caused by the size of Mg nanoparticles. Reprinted with permission from Ref. [93]. Copyright 2014, Royal Society of Chemistry.

After the particle size of the material has been reduced to the nanometer size, the specific surface area of the particles increases, resulting in a significant rise in active sites that can accelerate the dissociation of H_2 on the material surface. Additionally, the reduced particle size to the nanoscale shortens the diffusion path of H, making it more favorable to diffusion. Furthermore, the nanoscale particle size exposes most of the atoms to the surface after the material has completed hydrogen absorption, which can lead to the instability of the Mg-H bond and result in a lower hydrogen desorption temperature of the material.

2.1.3. Core–Shell Structure

Nanosizing significantly enhances the kinetic/thermodynamic performance of materials. Nevertheless, the sensitivity of nanoscale Mg-based materials to oxygen increases, making it challenging to store and transport them, which severely restricts their application fields and environments [45]. To preserve the excellent performance of nanoscale materials while mitigating their sensitivity to gas impurities, it is crucial to protect the materials' surface. The formation of the material surface shell layer presents an excellent solution to this

challenge. Typically, Mg-based materials with a core–shell structure are produced through ball milling, cladding, plasma, nano-confinement, and vapor deposition techniques.

High-energy ball milling is one of the most common methods for preparing nanomaterials with a core–shell structure [94,95]. Cui et al. [96] produced Mg-Ti core–shell structures with a maximum shell thickness of 10 nm via ball milling. The temperature-programmed desorption (TPD) and an isothermal hydrogen desorption analysis confirmed that the Mg-Ti material with a core–shell structure demonstrated outstanding hydrogen desorption properties, with an initial hydrogen desorption temperature of approximately 175 °C and a change in the entropy of the hydrogen desorption reaction (ΔS) from 130.5 to 136.1 J mol^{-1} K^{-1} H_2. Moreover, the equilibrium temperature at 0.1 MPa also decreased, leading to a lower initial hydrogen desorption temperature of the material. The shell layer contains multiple valence states of Ti, such as Ti(0), TiH_2(+2), $TiCl_3$(+3), and TiO_2(+4). A new mechanism of action has been put forward whereby multivalent Ti can act as a medium for electron transfer, which makes it easier for H_2 to recombine on the surface of the compound of Ti. The existence of such a mechanism can reduce the desorption temperature of MgH_2 and accelerate the hydrogen desorption process (Figure 7).

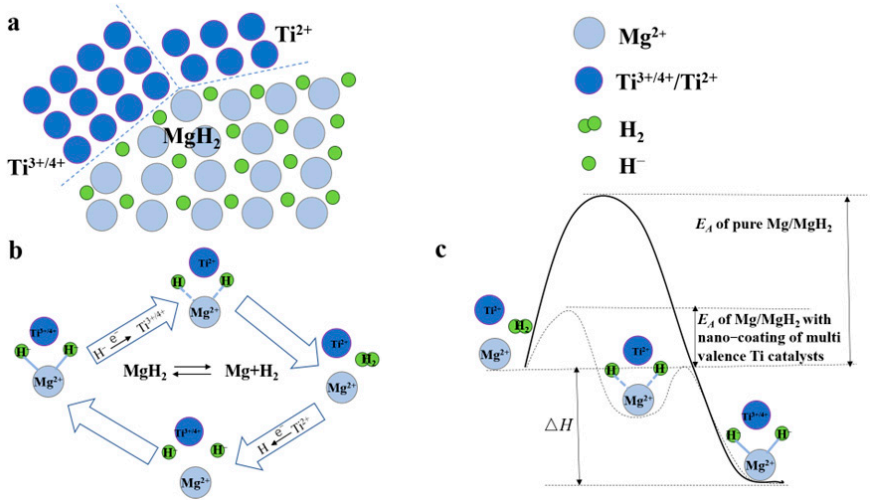


Figure 7. Many interfaces exist between MgH_2, high and low valent Ti compounds during hydrogen desorption of Ti−based multivalence catalyst−doped MgH_2 system (**a**), the multivalent Ti acts as an intermediate medium for electron transfer (**b**), the catalytic mechanism of multivalent Ti (**c**). Reprinted with permission from Ref. [96]. Copyright 2013, Royal Society of Chemistry.

Cladding is another method used to prepare Mg-based materials with a core–shell structure. Cui et al. [97] synthesized a series of Mg-TM (TM = Ti, Nb, V, Co, Mo, Ni) nanocomposites with a core–shell structure by covering Mg with transition metals, and these Mg-TM nanocomposites have excellent hydrogen desorption properties. Moreover, it was found that the Mg-TM composites prepared via cladding have better hydrogen storage performances than those prepared using the ball milling method, which is mainly due to the fact that the cladding treatment can make the Mg on the surface of the core particles fully contact with the transition metal in the shell layer and accelerate the diffusion rate of H (Figure 8). The peak temperature of hydrogen desorption of the Mg-TM sample was tested (Figure 9), revealing that Ti has the most significant effect on the dehydrogenation of MgH_2, lowering the desorption temperature by 150 °C compared to that of MgH_2. According to the analysis, the hydrogen desorption process of the material follows a redox mechanism. In this mechanism, the multivalent TM element acts as a mediator for electron transfer, which has a catalytic effect that accelerates the electron transfer and enables the material to complete the hydrogen desorption reaction swiftly.

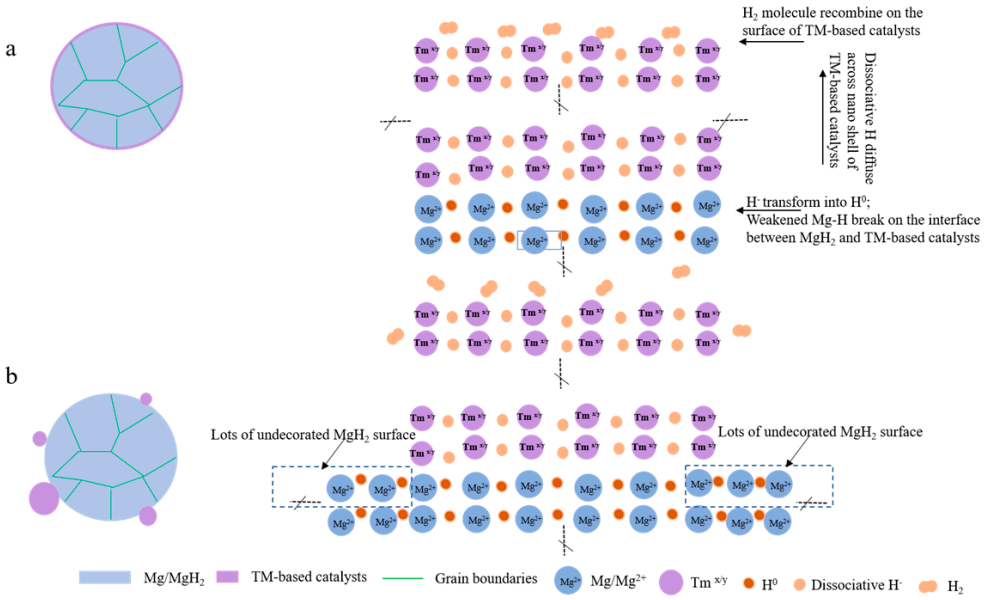


Figure 8. A section schematic of Mg−TM (**a**) and ball-milled Mg−TM−based catalyst (**b**). Reprinted with permission from Ref. [97]. Copyright 2014, Royal Society of Chemistry.

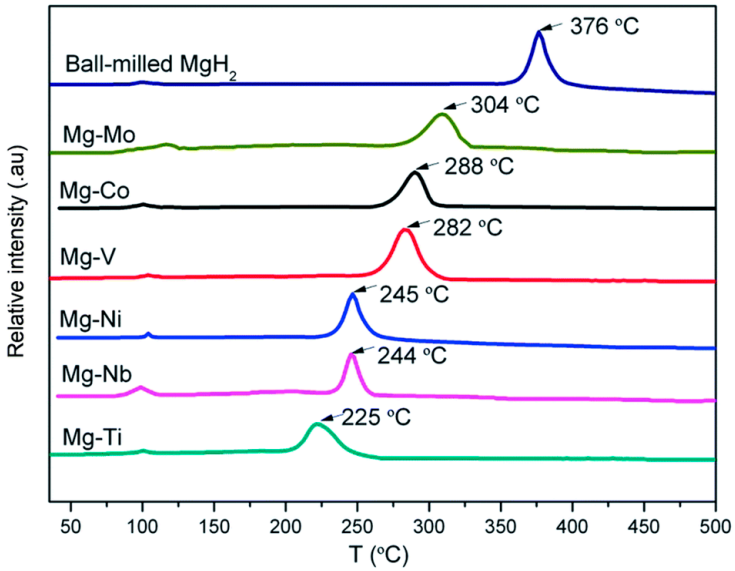


Figure 9. TPD-MS test curves of Mg−TM sample. Reprinted with permission from Ref. [97]. Copyright 2014, Royal Society of Chemistry.

Zou et al. conducted extensive research on Mg-based materials with a core–shell structure using the arc plasma method. In their study [98], Mg-based rare-earth nanocomposites (Mg-RE, RE = Nd, Gd, Er) were produced via the arc plasma method. An XRD analysis and TEM observation revealed that the ultrafine Mg (RE) particles within the Mg-RE composites were enveloped by nano-MgO and RE_2O_3, forming a distinctive core–shell-structured metal oxide composite. Among the materials, Mg-Er displayed the maximum decrease in hydrogen absorption enthalpy (8.7 kJ mol^{-1} H_2), with the high-temperature (400 °C) hydrogen storage capacity increasing from 6.24 to 7.37 wt%. The presence of the core–shell structure provided the Mg-RE composite powders with superior oxidation resistance, and the nano-RE_2O_3 in the core–shell structure had a catalytic effects on the hydrogen absorption reaction of the materials, contributing to the enhanced thermodynamic/kinetic performance of the ultrafine Mg particles. Mao et al. [99] prepared Mg-MF_x (M = V, Ni, La, Ce) nanocomposites with core–shell structures by mixing Mg powder with different

types of metal fluorides (VF_3, NiF_2, LaF_3, and CeF_3) using the arc plasma method. Moreover, Mg-NiF_2 had the best low-temperature hydrogen absorption performance, absorbing 3.26 wt% of H_2 in 2 h at 100 °C, while the Mg-VF_3 composite showed the greatest decrease in peak desorption temperature (by 41.8 °C). Metal fluoride reacts with Mg during the evaporation and condensation of arc plasma to form MgF_2 and transition metal particles, which cover the Mg surface and eventually form a core–shell-structured composite material (Figure 10). The surface shell structure of Mg-MF_x composites has a catalytic effect and can prevent the agglomeration of material particles, leading to improved hydrogen absorption/desorption performances.

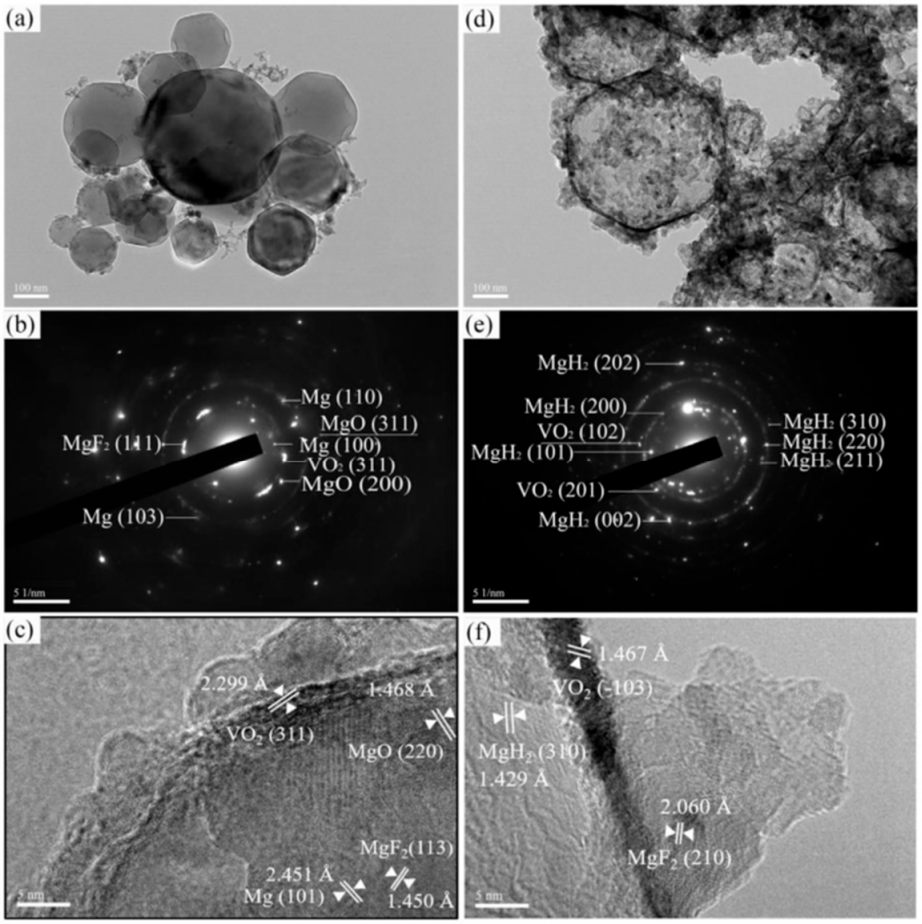


Figure 10. TEM images of the Mg-VF_3 powder (**a**), the SAED pattern (**b**), and the HRTEM image (**c**). A micrograph of the hydrogenated Mg−VF_3 powder (**d**), the SAED pattern (**e**), and the HRTEM image (**f**). Reprinted with permission from Ref. [99]. Copyright 2017, Elsevier.

Studies have demonstrated that transition metals, such as Ti, Fe, and Ni, exhibit a remarkable catalytic effect on the hydrogen absorption/desorption reaction of Mg-based materials [100]. Zou et al. [101] prepared Mg-TM-La ternary composite powder materials (TM = Ti, Fe, Ni) using the arc plasma method for the first time. They found that the ternary composite powder's main structure and phase composition were ultrafine Mg particles encapsulated by nano-La_2O_3 and MgO. The hydrogen absorption/desorption performance of the Mg-TM-La system was significantly improved when compared with that of the binary Mg-TM or Mg-La system, with a faster hydrogen absorption rate and a lower hydrogen desorption temperature (Figure 11). By adding a trace amount of transition metals (particularly Ti and Ni), along with La_2O_3, a significant improvement in the thermodynamic/kinetic performance of Mg-based materials can be achieved due to the excellent catalytic role played by these additives in the hydrogen absorption/desorption processes.

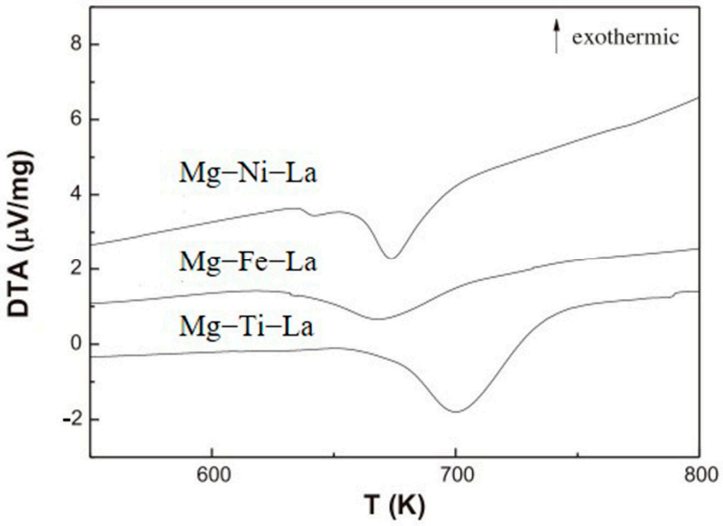


Figure 11. DTA curve of Mg−TM−La powder after hydrogen absorption. Reprinted with permission from Ref. [101]. Copyright 2013, Elsevier.

Zou et al. [102] also synthesized binary Mg@Ti and ternary Mg@Ti@Ni composites with core–shell structures using the arc plasma method and then investigated their microstructures and properties. After hydrogen absorption by the composites, it was observed that the materials had MgH_2 as the core and Ti or Mg-Ni hydride as the shell and that they had a rougher surface than pure Mg particles (Figures 12 and 13). The hydrogen absorption activation energy, enthalpy, and peak temperature of the hydrogen desorption of the ternary composites are lower than those of the binary composites, which is primarily attributed to the catalytic effect of TiH_2 and Mg_2Ni covering the surface of the Mg particles. Furthermore, TiH_2 as the active site and Mg_2Ni as the "hydrogen pump" can further accelerate the hydrogen absorption. The results show that the co-plating of Ti and Ni can further enhance the hydrogen absorption thermodynamics/kinetics of Mg (Figure 14).

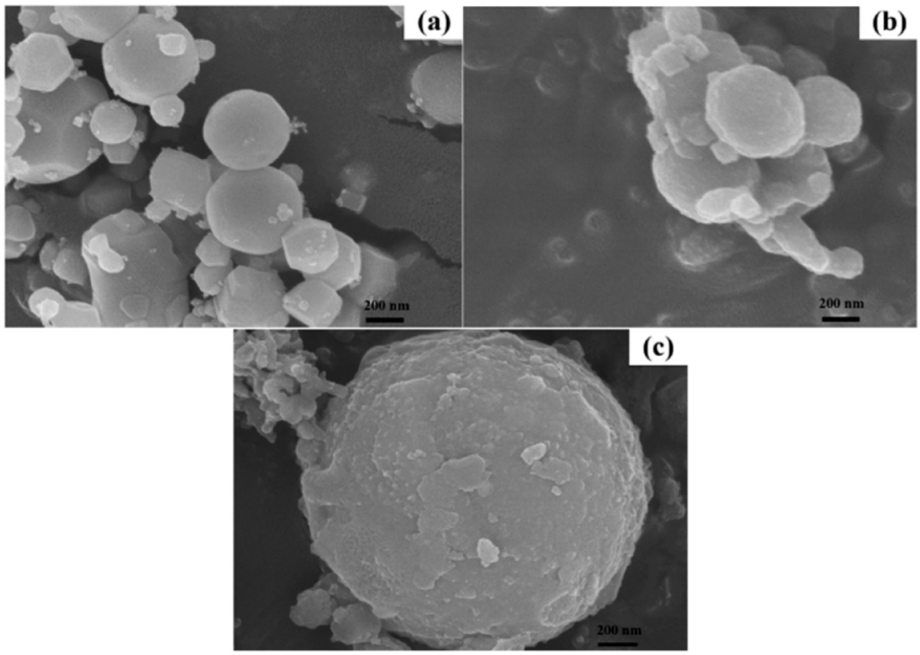


Figure 12. SEM images of pure Mg powder (**a**), Mg@Ti (**b**), and Mg@Ti@Ni composites (**c**). Reprinted with permission from Ref. [102]. Copyright 2017, Elsevier.

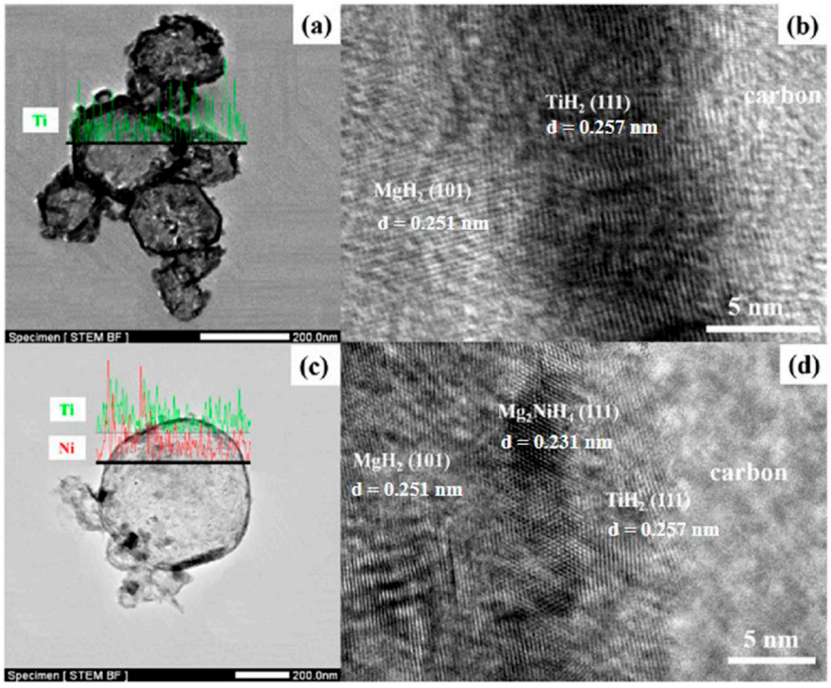


Figure 13. BF−STEM and HRTEM images of Mg@Ti (**a**,**b**) and Mg@Ti@Ni (**c**,**d**) composites after hydrogen absorption. Reprinted with permission from Ref. [102]. Copyright 2017, Elsevier.

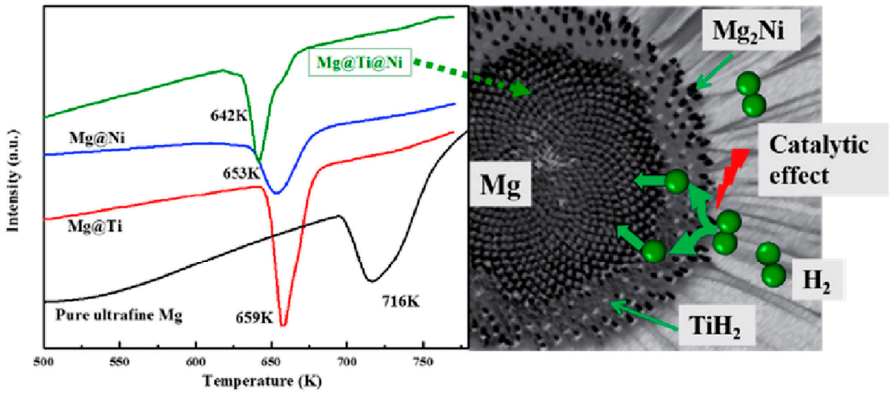


Figure 14. The peak dehydrogenation temperature of different materials and synergistic effects present in Mg@Ti@Ni composites. Reprinted with permission from Ref. [102]. Copyright 2017, Elsevier.

Based on the mechanism of the above optimizations for Mg-based ternary composites, Lu et al. [103] synthesized binary Mg@TM (TM = Co, V) and ternary Mg@Co@V composites with core–shell structures using a combination of the arc plasma and reduction methods. The enthalpy and activation energy required for the hydrogen absorption process of the ternary composite were lower than those of the binary materials and pure Mg, in addition to having a lower initial hydrogen desorption temperature. An analysis indicated that the properties of the material can differ depending on the type and quantity of phases present in the shell layer. Consequently, forming a core–shell structure with ternary composites can more significantly enhance the hydrogen absorption/desorption performance of the material. Jeon et al. [104] prepared Mg NCs/PMMA nanocomposites with core–shell structures using poly (methyl methacrylate) (PMMA) as the confinement material for metallic Mg nanocrystals (NCs). Mg particles over 60 wt% and 5–15 nm in diameter were dispersed in the polymer. The composite material had a fast hydrogen absorption/desorption ability below 200 °C. The use of PMMA in composite materials forms a gas-selective polymer barrier that enables the hydrogen absorption/desorption process while oxidation is prevented

(Figure 15). A TEM analysis revealed that Mg NCs embedded with PMMA had a spherical morphology and an average particle size of around 4.9 nm and were uniformly distributed. The polymer shell also serves as a protective and catalytic layer that prevents the oxidation and agglomeration of nano-Mg particles. Xia et al. [105] employed the nano-confinement method to prepare MgH_2-GR-Ni composites, where graphene acted as a structural support and spatial barrier to suppress the growth of MgH_2 nanoparticles. As a result, the activation energies for hydrogen absorption and desorption were reduced to 22.7 and 64.7 kJ mol^{-1} H_2, respectively, significantly improving the material's hydrogen storage properties. Callini et al. [106] synthesized Mg nanoparticles with a metal oxide shell morphology using inert gas condensation and modified them with in situ Pd deposition, where discontinuous layers with Pd clusters formed on the MgO shell. The presence of the MgO shell layer retarded the further oxidation of the composites, and the modification of Pd further improved the hydrogen absorption performance of the materials. Ma et al. [107] prepared a nanobox (CoS-NB) scaffold derived from a Co-based metal–organic framework (MOF) with a mesoporous structure. The nanosizing of MgH_2 within the porous structure of CoS-NBs was successfully achieved during the hydrogen absorption of the material. The unique core–shell structure and the "nanometer size effect" reduced the enthalpy of the hydrogen absorption/desorption of the composite material. At the same time, the generated MgS had a catalytic effect, which enhanced the kinetic properties of the material.

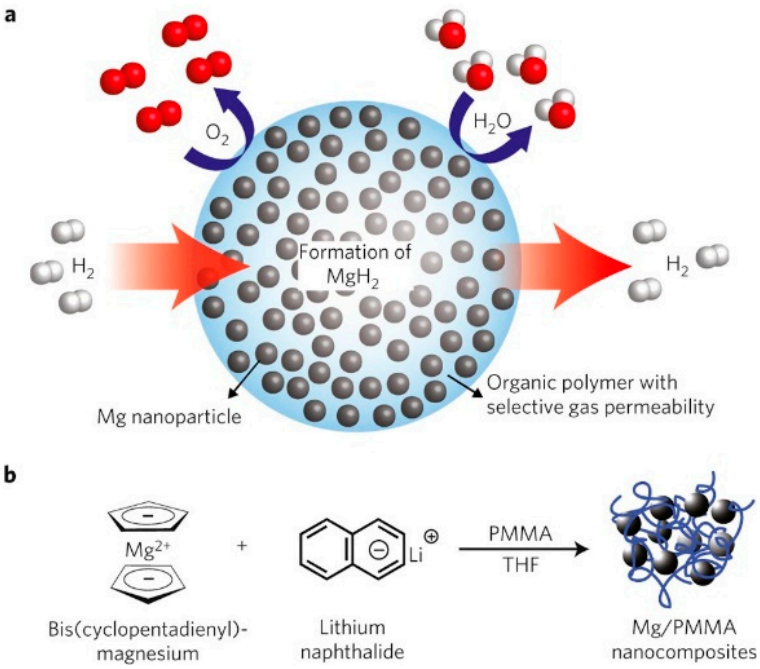


Figure 15. A schematic of high−capacity Mg NCs encapsulated by a selectively gas−permeable polymer (**a**), the synthesis of Mg NCs/PMMA nanocomposites (**b**). Reprinted with permission from Ref. [104]. Copyright 2011, Springer Nature.

A "shell" with a good catalytic effect can be formed on the surface of Mg-based materials by using different preparation and treatment methods. However, the underlying mechanism for improving the performance of these materials remains similar. The choice of the shell layer material is crucial, but most current studies have chosen nanoscale elemental particles and their compounds with catalytic effects. The catalytic effect of the shell layer can reduce the activation energy of hydrogen absorption/desorption, which leads to a lower absorption/desorption temperature and a faster absorption/desorption rate, and studies have shown that the multi-phase formation of the shell layer with better catalytic effect. In addition, the protective effect of the shell layer can also prevent the oxidation of Mg-based materials in contact with air and improve the cycle life of the materials.

The low cost, high hydrogen storage capacity, and abundant raw materials of Mg-based materials have made them a promising choice in the energy storage industry. However, the material's surface tends to form an oxide film that hinders the hydrogen absorption/desorption reaction, and the performance of hydrogen storage heavily relies on temperature conditions. The surface properties of the material play a crucial role in determining hydrogen storage characteristics, such as the absorption/desorption rate, temperature, and activation duration. This chapter has discussed various surface treatment methods, including surface catalytic treatment, nanocrystallization treatment, and the formation of core–shell structures, and their effects on the hydrogen storage performances of Mg-based materials. The introduction of the nanoscale catalytic phase allows it to provide more active nucleation sites for the surface reactions of the material. At the same time, the catalytic effect can also accelerate the rate of the hydrogen absorption/desorption reaction occurring. On top of this, graphite material is introduced, and the special porous structure of graphene can provide additional diffusion channels for H, thus creating a synergistic effect with catalysis and greatly reducing the time required for the reaction. Nanosizing treatment also boosts hydrogen storage performance by providing more active sites for H_2. At the same time, the refinement of the particles also creates shorter diffusion distances and more diffusion paths for H. These factors collectively promote faster hydrogen absorption rates. Reducing the particle size of catalysts is an effective way to improve their catalytic activity since catalyst activity is directly related to the number of catalytically active atoms on the surface of the carrier. A large number of studies have found that the incorporation of nanoscale catalysts in Mg-based materials with nanostructures can further improve the hydrogen storage properties of the materials compared to those of matrix materials without any treatment. A core–shell structure is mainly formed to protect the more "fragile" surface of the materials after nanocrystallization. This is carried out in order to maintain and further enhance the excellent hydrogen absorption/desorption performance of Mg-based materials. The current research has proved that a layer of catalytic "shell" can be formed by covering the catalyst on the surface of Mg particles with different preparation methods. This structure can play a catalytic role while protecting the surface of the material at the same time so that the material has a better hydrogen storage performance. It provides a very important method for the preparation of nanometer Mg-based materials with high catalytic and long-cycle abilities. The surface modification of Mg-based materials using various techniques can greatly enhance their kinetic and thermodynamic properties. In summary, although the various surface modification treatments differ in their methods and principles, they are also subtly related. The most direct manifestations for improving the hydrogen storage properties of the materials all lead to an increase in the hydrogen absorption/desorption rate, a decrease in the hydrogen absorption/desorption temperature, and a decrease in the material enthalpy and activation energy. In addition, different modification methods can be used as a reference for further research and improvement of material properties.

2.2. Surface Modifications of Electrode Materials in Nickel–Metal Hydride Batteries

Ni-MH batteries are secondary new energy batteries with $Ni(OH)_2$ as the positive electrode, metal hydride (MH) as the negative electrode, and an alkaline solution as the electrolyte (Figure 16a) [108,109]. Ni-MH batteries have been widely used in commercial hybrid vehicles, such as Toyota, Honda, and Ford, since 1999 due to their high level of safety, environmental friendliness, and good low-temperature properties [110,111]. However, the capacity, durability, and discharge performance (kinetics) of the battery depend primarily on the inherent properties of the electrode materials, especially for the preparation of active materials for the negative electrode [112,113]. There have been a series of studies on negative electrode materials for Ni-MH batteries, such as AB_5, AB_2, AB_3, AB, A_2B, and Mg-based materials [114–118]. However, with these materials for Ni-MH battery applications in the field of high power, there are still some problems, such as easy polarization, a

poor discharge ability at a high rate, easy corrosion in alkaline electrolytes, and poor cycling stability.

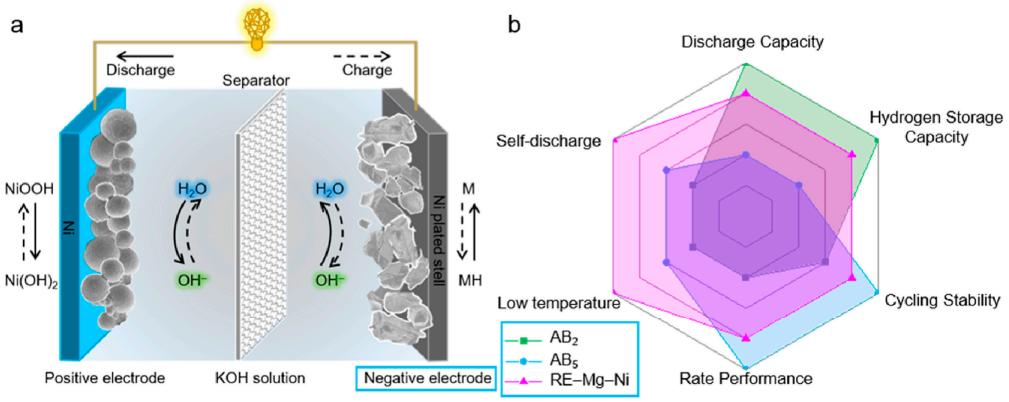


Figure 16. Schematic illustration of a Ni-MH battery (**a**) and radar chart comparison of AB_2-type, AB_5-type, and RE-Mg-Ni-based hydrogen storage alloys (**b**). Reprinted with permission from Ref. [108]. Copyright 2021, KeAi Publishing.

The performance of Ni-MH batteries depends not only on the bulk structure of the electrode but also on its surface state. Mg-based alloys are widely used as the negative electrode in Ni-MH batteries due to their exceptional electrochemical properties, cost-effectiveness, and abundant reserves of raw materials (Figure 16b) [108]. However, the appearance and growth of its $MgO/Mg(OH)_2$ surface layer impede electron transport at the electrode/electrolyte interface and create a large discharge potential, resulting in a lower discharge capacity and a poorer kinetic performance of the electrode material [119]. Moreover, the interfacial reaction between the electrode material and the electrolyte can seriously affect the electrochemical performance of the batteries [120,121]. The optimization of the performance of Mg-based electrode materials and Ni-MH batteries can be achieved through surface treatment. Common methods of modification include surface coating, nanocrystallization and amorphization, and surface catalysis.

2.2.1. Surface Coating

The cycling stability of a battery is an essential manifestation of the ability of the electrode materials to resist capacity decay. It is a critical factor in evaluating battery performance, which directly determines the suitability of the electrode material for the commercial applications of Ni-MH batteries. Surface coating treatment can create a new active surface and effectively enhance the electrochemical performance of Mg-based alloy electrodes [122]. It has been reported that the construction of metals (Cu, Ni, Co, and Pd) [123–125], reduced graphite oxide (rGO) [126], and certain polymer coatings [127] on the surface of alloys can act as electrocatalysis, anti-corrosion, and microcurrent conductors around the alloy particles, which can improve their electrochemical properties. The cycle life, anti-chalking, and corrosion resistance of the electrodes have been enhanced by the surface modification of Mg-based alloys with nano-metallic particles or conducting polymers [128–130].

Li et al. [131] conducted a study on a Mg-Nd-Ni alloy as a negative electrode material for Ni-MH batteries. They used chemical plating on the surface of a $Nd_{0.7}Mg_{0.3}Ni_3$ alloy, with Ni and Co plating treatments carried out separately (Figure 17). The research showed that the surface of the uncoated alloy powder was smooth, with only a few tiny particles formed during the material preparation process adhering to the surface. After the Ni or Co plating treatments, a modified layer was formed on the surface of the base alloy. Honeycomb Ni and flaky Co were deposited on the alloy surface. However, the Ni plating was found to form a denser and more stable metal coating on the surface of the base alloy than the Co plating (Figure 18). Electrochemical tests revealed that both coatings exhibited high electrocatalytic activity during the electrode reaction, promoting

the charge transfer on the electrode surface. The surface modification resulted in an improvement in the initial discharge capacity of the electrode material, as well as good high-rate discharge performances. At a discharge current density of 1800 mA g^{-1}, the high-rate discharge increased by 20.4% (Ni coating) and 18.3% (Co coating), and the two coatings still maintained good integrity on the surface of the alloy after 100 charge/discharge cycles, resulting in a good corrosion resistance of the electrode in alkaline electrolytes.

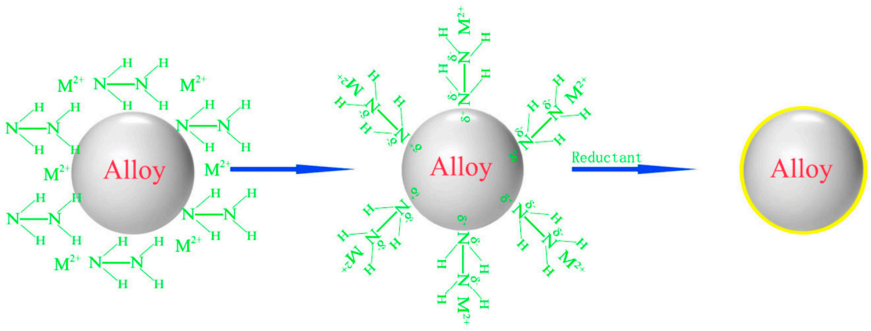


Figure 17. Formation of alloy surface coating. Reprinted with permission from Ref. [131]. Copyright 2017, Elsevier.

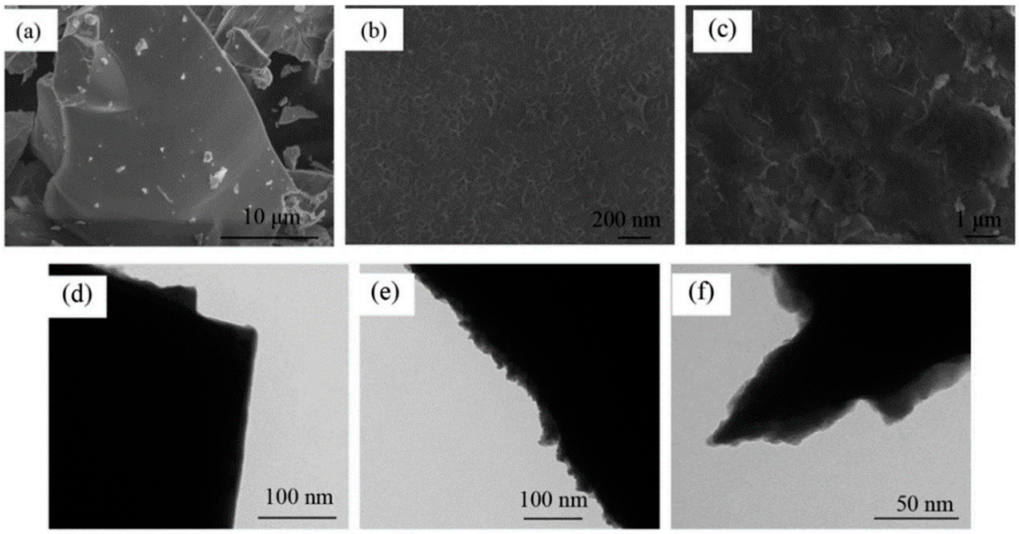


Figure 18. Morphology of alloy powders before and after electroless plating. (**a**) Untreated alloy SEM; (**b**) Ni-coated alloy SEM; (**c**) Co-coated alloy SEM. (**d**) Untreated alloy TEM; (**e**) Ni-coated alloy TEM; (**f**) Co-coated alloy TEM. Reprinted with permission from Ref. [131]. Copyright 2017, Elsevier.

Du et al. [132] synthesized an rGO-Mg_2Ni composite by successfully coating reduced graphene oxide (rGO) on the surface of a Mg_2Ni alloy with an amorphous structure to enhance the cycling stability of Mg_2Ni as an electrode material (Figure 19). The material has a capacity of 557 m Ah g^{-1} after the 10th cycle, with a capacity retention rate of up to 94%. After 50 cycles, the capacity can also be maintained at 60%, which is significantly improved compared with the untreated Mg_2Ni material. In addition, a Tafel polarization test of the electrode showed that the electrode material has high corrosion resistance in an alkaline solution (Figure 20). The structure of graphene provides a high-quality barrier that prevents direct contact between the hydroxyl groups in the alkaline electrolytes and the electrode during the charging/discharging process. The reduced graphene oxide coating treatment also accelerated the charge transfer and ion diffusion on the surface of Mg_2Ni.

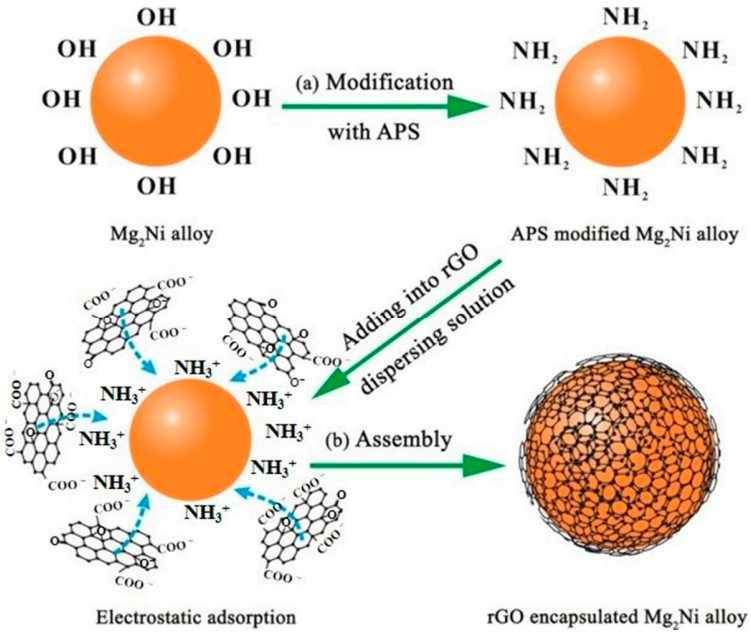


Figure 19. The preparation process of rGO−Mg_2Ni: (**a**) APS modification; (**b**) electrostatic self-assembly. Reprinted with permission from Ref. [132]. Copyright 2017, American Chemical Society.

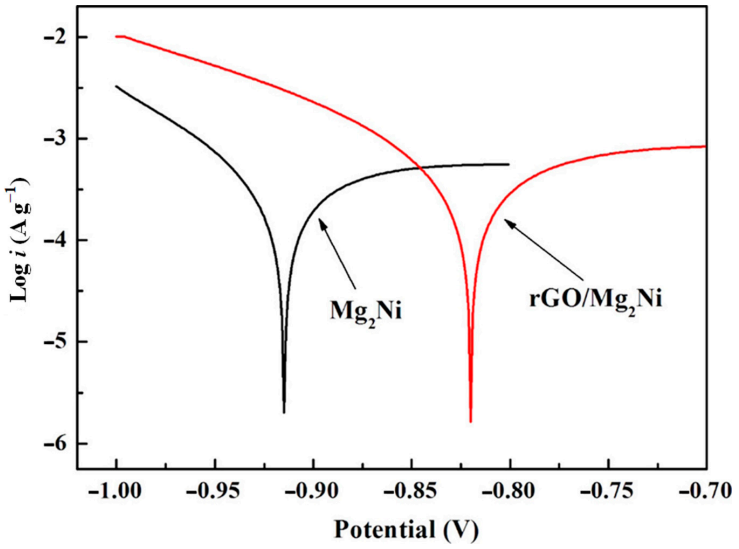


Figure 20. Tafel polarization curves of the bare Mg_2Ni alloy and rGO−Mg_2Ni composite electrodes (scan rate: 1 mV s^{-1}). Reprinted with permission from Ref. [132]. Copyright 2017, American Chemical Society.

Studies have explored surface coating modifications for Mg-based alloys. These include the formation of Ni-Cu-P coatings on the surface of La-Mg-Ni as a base material [133], as well as the coating of La-Mg-based electrode materials with various Ni-based compounds using different methods [134,135]. Santos et al. [136] investigated the effect of two mechanical coatings (Ni and Ni + 5 wt% Al) on the structure, powder morphology, and electrochemical performance of a Mg + 50 wt% Ni alloy. It was found that the maximum discharge capacity of the Mg-Ni alloy was 211 mA h g^{-1} and that the two mechanical coatings could further increase this to 257 mA h g^{-1} (Ni coating) and 273 mA h g^{-1} (Ni + 5 wt%Al coating), respectively, as well as improving the cycle life of the electrode material. Although a mechanical coating on the material surface can enhance the electrochemical performance of electrode materials and batteries to a large extent, it is still far from meeting the require-

ments of everyday life and practical industrial applications. Therefore, a large number of experiments have been carried out to study and analyze the effects of different surface modification mechanisms on the electrochemical performances of Mg-based materials; additionally, more straightforward, economical, and effective surface treatment methods are currently being explored.

The study above highlights the importance of a surface coating on electrode materials. It serves the dual role of electrocatalysis and protection, facilitating charge transfer during electrode reactions and providing protection against rapid corrosion by the electrolyte. Despite the benefits of a mechanical coating in improving electrochemical performance, such as providing a better high-rate discharge performance, initial discharge capacity, and capacity retention, it falls short of practical application requirements in the industry. Therefore, researchers are exploring various surface modification mechanisms and more superficial, more economical, and effective surface treatment methods to enhance the performance of Mg-based materials and batteries.

2.2.2. Nanocrystallization and Amorphization

Materials synthesized via different preparation processes also tend to differ significantly in their properties. In terms of the nanocrystalline and amorphous processing of alloying materials, mechanical grinding is recognized as an effective method to prepare Mg-based materials with nanocrystalline or amorphous structures. Moreover, it has been shown that the grain size of the materials decreases significantly with an increasing grinding time [137,138].

Tian et al. [139] prepared amorphous $Mg_{0.9-x}Ti_{0.1}Pd_xNi$ (x = 0.04–0.1) materials by using the mechanical grinding method. The results showed that replacing Mg with Pd greatly improves the cycling stability of the electrode, as well as the resistance to corrosion in KOH solutions and the surface resistance to oxidation. By comparing and analyzing the cycle capacity retention rate (C_{20}/C_1, C_{50}/C_1) of the $Mg_{0.9-x}Ti_{0.1}Pd_xNi$ (x = 0.04–0.1) electrode, it was found that the cycle stability of the electrode was significantly enhanced (Table 1). When x was 0.1, the alloy electrode could still maintain a discharge capacity of more than 200 mA h g^{-1} after 80 cycles. It was concluded from the experimental analysis that the improved electrode properties are due to the formation of a passivation film composed of oxides such as $Mg(OH)_2$, TiO_2, NiO, and PdO on the material surface, and the thickness of the passivation film and the hydrogen diffusion coefficient will increase with the increase in the Pd content in the material.

Table 1. The discharge capacities and cyclic stability of the $Mg_{0.9-x}Ti_{0.1}Pd_xNi$ (x = 0–0.1) electrode alloys. Reprinted with permission from Ref. [139]. Copyright 2006, Elsevier.

x	MDC (mA h g^{-1})	CRR C_{20}/C_1 (%)	CRR C_{50}/C_1 (%)	C_n > 200 mA h g^{-1} (Cycle Number)
0	455	31.6	-	-
0.04	390.7	66.7	-	46
0.06	366.5	69.4	59.9	67
0.08	343.9	77.8	64.8	77
0.1	326.5	74.2	67.2	80

Note: (1) MDC indicates the maximum discharge capacity, and CRR indicates the capacity retention rate (C_n indicates the capacity after the nth cycle). (2) "-" indicates that no data exist.

Zhang et al. [140] prepared a $La_9CeMg_{80}Ni_5$ alloy using a high-purity helium vacuum induction furnace. They synthesized the $La_9CeMg_{80}Ni_5$ + 200 wt% Ni + x wt% GR (x = 0–4) composites with nanocrystalline and amorphous structures by using mechanical nickel and graphite (GR) plating operations on the surface of the alloy. The results showed that adding GR and increasing the ball milling time could improve the electrochemical properties of the composites, increasing the discharge capacity, cycling stability, and electrochemical kinetics of the composites, while the optimal content of GR was determined to be x = 3. When the GR percentage was increased from 0 to 3, the initial discharge capacity of the

material increased from 288.1 to 315.4 mA h g^{-1} after carrying out ball milling for 20 h and from 314.5 to 344.9 mA h g^{-1} after carrying out ball milling for 80 h (Figure 21). After analyzing the data from the structural and performance tests, they believed that the improved cycling stability resulting from adding GR was due to the graphite layer formed on the electrode surface. A graphite layer has high electrocatalytic activity and can significantly promote the formation of a large number of nanocrystalline and amorphous structures, which also have a protective effect preventing the oxidation of the alloy surface and inhibit the corrosion of the electrode by the electrolyte. The incorporation of Fe, Zn, and Ti has been studied and proven to improve the properties of the base metal [141–143]. However, there are few reports on the substitution with V. In order to study the effect of V content on the performances of materials, Bu et al. [144] prepared amorphous and nanocrystalline $Mg_{50-x}V_xNi_{45}Fe_3Zn_2$ (x = 0–4) + 50 wt% Ni alloys by using mechanical ball milling and surface nickel plating. The results show that the nickel layer can not only restrain the corrosion of the electrode but that it also has good electrocatalytic performances. In addition, the alloy exhibits active electrochemical performances at room temperature. With an increase in ball milling time and V content, electrode materials' discharge capacity and cycle stability are significantly improved.

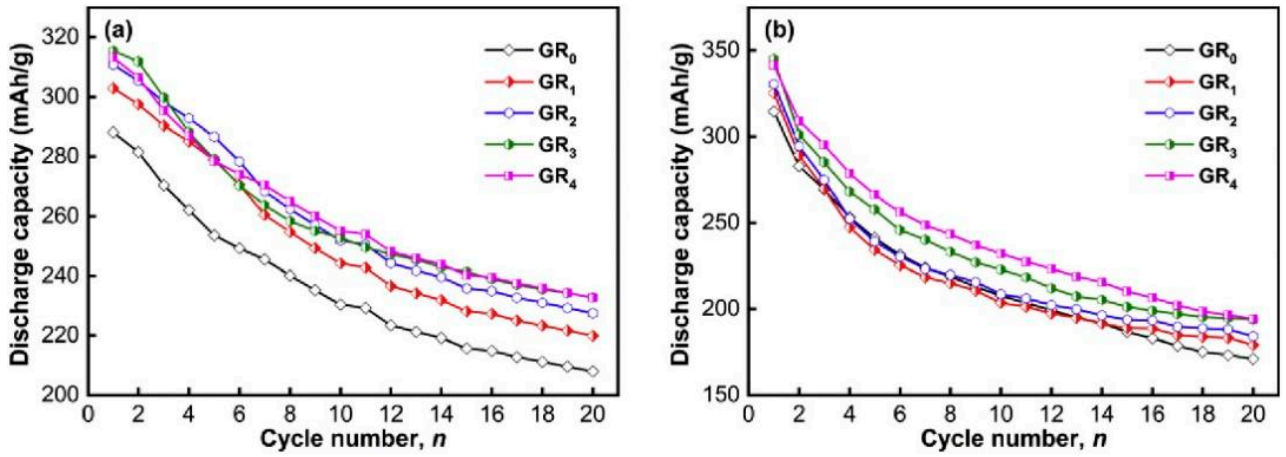


Figure 21. Evolution of the discharge capacity of the as-milled $La_9Ce_1Mg_{80}Ni_5$ + 200 wt% Ni + x wt% GR (x = 0–4) with cycle number: (**a**) Milling for 20 h, (**b**) milling for 80 h. Reprinted with permission from Ref. [140]. Copyright 2020, Elsevier.

According to the current study, the formation of nanocrystallization and amorphous structures of Mg-based materials is mainly achieved by the material preparation process (ball milling), and it is shown that the increase in ball milling time not only facilitates the formation of these two structures but also has a great influence on the material properties. Some additive materials (Pd, Fe, V, and graphite) can further enhance Mg-based material properties. For example, the addition of graphite facilitates the formation of nanocrystalline and amorphous structures during the ball milling process and passivation layers on the material's surface, and graphite has a certain electrocatalytic activity. Combined with the structure of the base material, it can further improve the material's initial discharge capacity, cycling stability, and corrosion resistance.

2.2.3. Surface Catalytic Treatment

Unwanted oxide layers usually form on the surface of Mg-based materials synthesized through melting or annealing. These layers hinder electrochemical reactions on the electrode surface during use as an electrode material. To improve surface catalytic activity and enhance electrochemical kinetics and discharge capacity, various methods such as acid/base treatment, heavy ion irradiation, and reduction atmospheres have been reported to effectively remove these oxide layers [145–148]. The use of the ball milling technique allows for the attachment of metals with certain catalytic properties to the surface

of Mg-based alloys, thus improving the composition and state of the alloy surface. During the ball milling process, the surface organization, structure, and grain size of the alloy are changed, which has a positive effect on improving the surface activity of alloys, preventing oxidation and inhibiting capacity losses [149,150].

It has been established that rare-earth oxides can be introduced as catalysts on the surface of Mg-based alloys to improve hydrogen storage properties. Zhang et al. [151] used $La_{1.7}Mg_{1.3}Ni_9$ alloy particles with a particle size of 25–45 μm as the base material, and then they introduced a trace amount of Y_2O_3 powder (50:1 mixture) via ball milling. Electrochemical tests revealed that, with an increase in the ball milling time, a nano-amorphous Y_2O_3 layer was generated on the surface of the alloy, which led to a significant increase in the electrochemical cycling stability of the material, as well as providing better corrosion resistance (Figure 22).

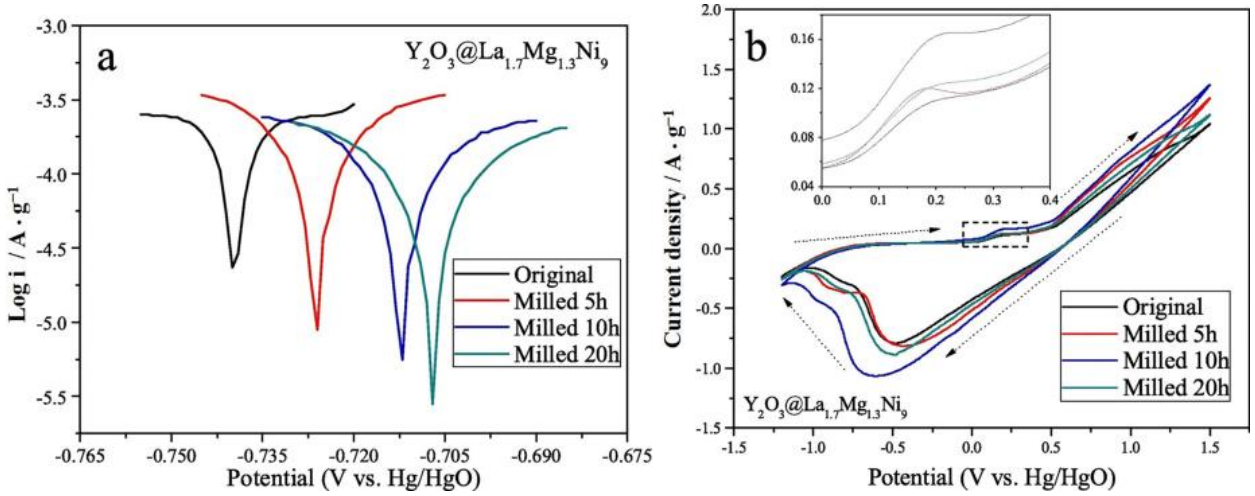


Figure 22. Tafel (**a**) and cyclic voltammetry curves (**b**) of the alloys. Reprinted with permission from Ref. [151]. Copyright 2020, Elsevier.

To enhance the electrochemical performance of alloy electrodes in alkaline electrolytes, surface pretreatment of the alloy with alkaline solutions is also an effective method. A $LaNi_{2.5}Co_{2.5}$ alloy was pretreated with KOH to study the electrode reaction kinetics [152]. The alloy was first treated with a hot KOH solution and then with a metallic nickel coating for dual surface modification [153]. A $LaNi_{4.7}Al_{0.3}$ electrode was treated with a $Co(OH)_2$-KOH solution to study its electrochemical properties [154]. After the alkali solution treatment, the contact resistance between the alloy particles and the charge transfer resistance at the electrolyte and electrode contact interface significantly decreased, leading to faster activation rates and a longer cycle life of the electrodes. Xiao et al. [155] systematically studied the effect of a KOH solution and KBH_4 solution treatment on the organization of a $La_{0.7}Mg_{0.3}Ni_{2.4}Co_{0.6}$ alloy and electrochemical properties. SEM tests showed that the surface of the alloy before treatment was very rough and resembled dense flower petals. The treatment with an alkaline solution resulted in a lamellar structure of the treated specimens with a distinct fracture shape and a wide size distribution. Electrochemical tests showed that the cyclic stability of the alloy electrode greatly improved following the alkaline solution treatment (Figure 23a). Moreover, it was obvious that the KBH_4 and KOH mixture had a better effect on the surface treatment of the material. The cyclic voltametric curves of the electrode materials are represented (Figure 23b) by the better kinetic properties of the treated materials (the height of the peak reflects the kinetic properties of the electrode [156]). The surface oxide layer of the material was effectively removed by the alkaline solution, which led to an enhanced diffusion rate of the ions within the alloy material and a decreased electrode charge transfer resistance. It was confirmed that surface pretreatment with an alkaline solution significantly improved the cycling durability of Ni-MH batteries.

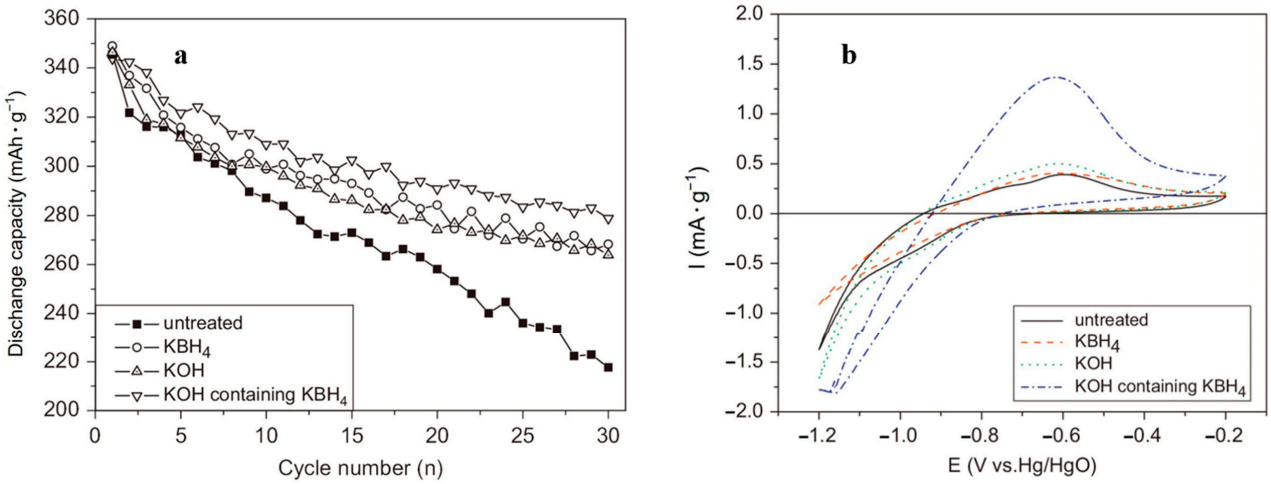


Figure 23. The cyclic life curves (**a**) and the cyclic voltammogram (CV) curves (**b**) of the $La_{0.7}Mg_{0.3}Ni_{2.4}Co_{0.6}$ alloy electrodes. Reprinted with permission from Ref. [155]. Copyright 2008, Elsevier.

Mg-based materials are seen as one of the best options for the preparation of negative electrode materials for Ni-MH batteries due to their abundant reserves and relatively low price. This section provides a brief overview of the impact of surface modification on the electrochemical performance of the electrode material and battery when Mg-based materials were used to prepare the negative electrode of Ni-MH batteries. Various surface modification methods for Mg-based materials, including surface coatings, nanocrystallization and amorphization, and surface catalytic treatment, are described, demonstrating that these modification techniques can enhance the electrochemical performance of electrode materials and batteries to a certain degree. The mechanisms related to the enhancement of the electrochemical properties of the materials after surface modification treatment are briefly analyzed. Surface coating treatment involves the application of a coating material on the surface of Mg-based materials to create a fresh active surface. Studies have shown that many coating materials, including transition metals and graphene, can enhance the electrochemical properties of electrodes. Both materials can improve the charge transfer rate during battery charging and discharging while preventing direct contact between the electrode materials and alkaline electrolytes. Surface catalytic treatments, however, involve attaching the catalyst material to the surface of Mg-based materials or enhancing the catalytic activity of the material surface through solution treatment. Although the principles behind these two methods differ, both can reduce charge transfer resistance, improve the tolerance of electrode materials in alkaline electrolytes, and enhance the cycling stability of electrode materials. The nanocrystallization and amorphization treatment mechanisms for enhancing the performance of Mg-based materials can be briefly summarized as follows: The formation of nanocrystals significantly increases the grain boundary area, providing more diffusion paths for ions. It also promotes the charge transfer ability of the electrode surface, thereby accelerating the electrode reaction processes. Although the modification mechanisms of the three methods are quite different, all of these treatment methods improve the performance of electrode materials to a certain extent. These different modification mechanisms provide a reference direction for future studies on improving the performances of Mg-based materials for further applications in industries.

2.3. Analysis of the Application of Magnesium-Based Materials in Existing Fields

The research and development of energy storage materials are crucial to the utilization and storage of energy. The ideal energy storage materials for a wide range of industrial and residential should consider factors such as the raw material and preparation costs, energy storage capacity, operating conditions, and service life. Mg has abundant reserves (about 2% [157]) and good hydrogen storage properties in the Earth's crust. Currently, the research on the performance of Mg-based materials in hydrogen storage mainly focuses

on solid-state hydrogen storage and Ni-MH batteries. Although researchers have shown that Mg-based materials show relatively excellent performance in hydrogen storage and electrochemical energy storage, which still not enough to achieve large-scale adoption.

In accordance with what is described in this paper, Tables 2 and 3 briefly summarize the relevant properties of some modified Mg-based materials in the field of hydrogen storage and Ni-MH batteries, respectively.

Table 2. Partial hydrogen storage properties of Mg-based materials after surface modification.

Materials	Surface Treatment	ΔH_{de} (kJ mol^{-1})	Capacity (wt%)	T_{ab} (°C)	T_{de} (°C)	Ref.
Mg	-	74.5	7.6	-	420	[158]
Mg	Surface catalytic phase (Ni@rGO)	-	6.0	-	300	[61]
Mg	Surface catalytic phase (Co@CNTs)	-	6.89	-	300	[62]
Mg	Surface catalytic phase (Fe_3O_4@GS)	60.62	6.20	290	-	[64]
Mg	Surface catalytic phase ($LiCoO_2$)	48.5	5.5	250	-	[159]
Mg_2FeH_6	Nanoparticles (<20 nm)	74	5.2	-	355	[76]
$La_7Sm_3Mg_{80}Ni_{10}$	Nanostructure	74.23	3	300	-	[74]
Mg-Ti	Nanoparticles (<32 nm)	71.3	5.2	-	190	[79]
Mg-Ti	Core–shell structure	-	5	-	250	[96]
Mg	Core–shell structure (Mg-Er)	69.9	7.37	-	-	[98]
Mg	Core–shell structure (Mg NCs-PMMA)	-	5.97	200	-	[104]
Mg	Core–shell structure (Mg-NiF_2)	-	3.85	200	-	[99]
Mg	Core–shell structure (Mg@Co@V)	74.83	-	-	323	[103]

Note: (1) The subscript ab indicates hydrogen absorption, and the subscript de indicates hydrogen desorption. (2) "-" indicates that no data exist.

Table 3. Partial electrochemical properties of Mg-based materials after surface modification.

Materials	Surface Treatment	MDC (mA h g^{-1})	CRR C_n/C_1(%)	ECD (mA g^{-1})	Ref.
$Nd_{0.7}Mg_{0.3}Ni_3$	Coating layer (Ni)	355	79.6 (C_{200})	202.6	[131]
$Nd_{0.7}Mg_{0.3}Ni_3$	Coating layer (Co)	337	76.5 (C_{200})	163.6	[131]
$La_{0.8}Mg_{0.2}Ni_{3.4}Al_{0.1}$	Coating layer (polyaniline)	391.8	87.5 (C_{100})	98.9	[129]
Mg_2Ni	Coating layer (rGO)	594	60 (C_{50})	225.9	[132]
Mg_2Ni	Coating layer (Ni)	946	38 (C_{10})	91.6	[128]
$Mg_{0.9}Ti_{0.1}Ni$	-	455	31.6 (C_{20})	-	[139]
$Mg_{0.8}Ti_{0.1}Pd_{0.1}Ni$	Amorphous structure	326.5	74.2 (C_{20})	184	[139]
$La_9Ce_1Mg_{80}Ni_5$(Ni + 3 wt% GR)	Nanocrystalline and amorphous structures (ball milling 20 h)	315.4	73 (C_{20})	-	[140]
$La_9Ce_1Mg_{80}Ni_5$(Ni + 3 wt% GR)	Nanocrystalline and amorphous structures (ball milling 80 h)	344.9	55 (C_{20})	-	[140]
$La_{0.88}Mg_{0.12}Ni_{2.95}Mn_{0.10}Co_{0.55}Al_{0.10}$	Surface catalytic phase (Ni-Cu-P)	361	84.8 (C_{200})	378.9	[133]
$La_{0.75}Mg_{0.25}Ni_{3.2}Co_{0.2}Al_{0.1}$	Surface catalytic phase (Cu-Pd)	386.3	82.7 (C_{100})	483.8	[28]
$La_{1.7}Mg_{1.3}Ni_9$	Surface catalytic phase (Y_2O_3, milled 10 h)	392.2	90 (C_{30})	-	[151]
$La_{1.7}Mg_{1.3}Ni_9$	Surface catalytic phase (Y_2O_3, milled 20 h)	387	95 (C_{30})	-	[151]

Note: (1) MDC indicates the maximum discharge capacity, CRR indicates the capacity retention rate, and ECD indicates the exchange current density (C_n indicates the capacity after the nth cycle). (2) "-" indicates that no data exist.

Based on the current research, it can be found that, in the field of solid-state hydrogen storage, pure Mg materials have the highest hydrogen storage capacity. However, hydrogen absorption/desorption requires exceptionally high temperatures, which requires much energy consumption for assistance. The current research aims to improve the comprehensive performance of the material by improving the preparation method, changing the material composition and structure, and modifying the treatment method. The hydrogen storage properties of Mg-based materials can be improved to some extent after modification treatment, but this is limited to experimental data. As for the design of solid-state hydrogen storage systems, although many studies on hydrogen storage materials and systems already exist, there is a severe lack of practical industrial application validation due to technical and environmental constraints, and there is an extreme lack of research on large-scale hydrogen storage devices. Therefore, more attention should be paid to the local performance and practical applicability of the materials in future research, and practical application verification should be performed. Meanwhile, better preparation processes and modification technologies should be explored to accelerate the realization of large-scale, normalized, and multi-field applications of solid-state hydrogen storage systems.

Even though secondary batteries have a specific research and application base in electrochemical energy storage, further research on high-performance electrode materials is still essential to enhance battery performance. It has been found that, when Mg-based materials are used as anode materials for Ni-MH batteries, modification treatment can improve the corrosion resistance of electrode materials, but there are still apparent deficiencies in discharge capacity and high-rate discharge performance, which limits the application of the materials in the field of high-power batteries.

3. Conclusions and Prospects

Mg-based materials are considered key materials for potential applications in hydrogen storage and transportation, Ni-MH batteries, etc. However, the oxide layer on the material's surface can hinder the decomposition of H_2 and the penetration and diffusion of H. Furthermore, the active surface is susceptible to external factors, such as impurity gases and electrolyte corrosion. These problems impede the practical application of Mg-based materials in the field of energy storage. Surface modification is an effective method to improve the hydrogen storage and electrochemical performance of Mg-based materials. Based on two application scenarios of Mg-based materials as a hydrogen storage medium and an electrode material, this paper summarized and analyzed surface modification treatment methods, such as surface catalytic treatment, nanocrystallization and amorphization treatment, surface coatings, and the formation of a shell structure. The rate of hydrogen absorption/desorption, cycle life, corrosion resistance, and electrical conductivity of Mg-based materials are closely related to the surface state of the materials.

The performance of Mg-based materials in terms of hydrogen absorption/desorption and electrochemical performance in Ni-MH batteries can be significantly enhanced through surface modification treatments. Following the modification treatment, the hydrogen absorption/desorption kinetics and thermodynamics of Mg-based materials can be remarkably improved, resulting in an increased hydrogen absorption/desorption rate and a reduced hydrogen absorption/desorption temperature. For Mg-based Ni-MH electrode materials, surface modification treatment improves electrical conductivity, corrosion resistance, and cycle life, leading to a higher initial discharge capacity and better cycle stability as a manifestation of the enhanced electrochemical performance.

The widespread application of Mg-based materials is contingent on the stable production of these materials on a large scale. Currently, the surface modification method involves coating the surface of Mg-based materials with nanoscale materials possessing catalytic properties, resulting in the formation of a distinctive "shell" structure. This method is both straightforward to implement and controllable, with potential for industrial scaling. Moving forward, in addition to developing new surface modification methods, the existing methods need to be further investigated and integrated into the actual Mg-based

material production process to facilitate large-scale production and applications. In future studies, it is important to not only develop new techniques for modification but to also summarize and conduct in-depth studies to incorporate current methods into the practical scale production process of Mg-based materials, enabling improvements in the material's performance while expanding its application area.

Author Contributions: Conceptualization, Y.K., K.Z. and X.L.; validation, Y.K. and K.Z.; writing—original draft preparation, Y.K. and X.L.; writing—review and editing, Y.K.; visualization, K.Z. and X.L.; supervision, K.Z. and X.L.; project administration, K.Z. and X.L.; funding acquisition, K.Z. All authors have read and agreed to the published version of the manuscript.

Funding: This work was supported by the National Natural Science Foundation of China (Grant No. 52271062 and Grant No. 52201266) and the National Key R&D Program of China (Grant No. 2022YFB3803700).

Institutional Review Board Statement: Not applicable.

Informed Consent Statement: Not applicable.

Data Availability Statement: Not applicable.

Conflicts of Interest: The authors declare no conflict of interest.

References

1. Yang, Z.; Zhang, J.; Kintner-Meyer, M.C.; Lu, X.; Choi, D.; Lemmon, J.P.; Liu, J. Electrochemical energy storage for green grid. *Chem. Rev.* **2011**, *111*, 3577–3613. [CrossRef]
2. Li, K.; Bian, H.; Liu, C.; Zhang, D.; Yang, Y. Comparison of geothermal with solar and wind power generation systems. *Renew. Sustain. Energy Rev.* **2015**, *42*, 1464–1474. [CrossRef]
3. Khojasteh, D.; Khojasteh, D.; Kamali, R.; Beyene, A.; Iglesias, G. Assessment of renewable energy resources in Iran; with a focus on wave and tidal energy. *Renew. Sustain. Energy Rev.* **2018**, *81*, 2992–3005. [CrossRef]
4. Hussain, A.; Arif, S.M.; Aslam, M. Emerging renewable and sustainable energy technologies: State of the art. *Renew. Sustain. Energy Rev.* **2017**, *71*, 12–28. [CrossRef]
5. Pareek, A.; Dom, R.; Gupta, J.; Chandran, J.; Adepu, V.; Borse, P.H. Insights into renewable hydrogen energy: Recent advances and prospects. *Mater. Sci. Energy Technol.* **2020**, *3*, 319–327. [CrossRef]
6. Rosen, M.A.; Koohi-Fayegh, S. The prospects for hydrogen as an energy carrier: An overview of hydrogen energy and hydrogen energy systems. *Energy Ecol. Environ.* **2016**, *1*, 10–29. [CrossRef]
7. Pearson, P.J.G.; Foxon, T.J. A low carbon industrial revolution? Insights and challenges from past technological and economic transformations. *Energy Policy* **2012**, *50*, 117–127. [CrossRef]
8. Tarhan, C.; Çil, M.A. A study on hydrogen, the clean energy of the future: Hydrogen storage methods. *J. Energy Storage* **2021**, *40*, 102676. [CrossRef]
9. Zhang, F.; Zhao, P.; Niu, M.; Maddy, J. The survey of key technologies in hydrogen energy storage. *Int. J. Hydrogen Energy* **2016**, *41*, 14535–14552. [CrossRef]
10. Liu, C.; Li, F.; Ma, L.P.; Cheng, H.M. Advanced materials for energy storage. *Adv. Mater.* **2010**, *22*, E28–E62. [CrossRef]
11. Ibrahim, H.; Ilinca, A.; Perron, J. Energy storage systems–Characteristics and comparisons. *Renew. Sustain. Energy Rev.* **2008**, *12*, 1221–1250. [CrossRef]
12. Mahlia, T.M.I.; Saktisahdan, T.J.; Jannifar, A.; Hasan, M.H.; Matseelar, H.S.C. A review of available methods and development on energy storage; technology update. *Renew. Sustain. Energy Rev.* **2014**, *33*, 532–545. [CrossRef]
13. Song, Z.; Zhan, H.; Zhou, Y. Polyimides: Promising energy-storage materials. *Angew. Chem. Int. Ed.* **2010**, *49*, 8444–8448. [CrossRef] [PubMed]
14. Wang, T.; Chen, H.C.; Yu, F.; Zhao, X.S.; Wang, H. Boosting the cycling stability of transition metal compounds-based supercapacitors. *Energy Storage Mater.* **2019**, *16*, 545–573. [CrossRef]
15. Li, J.; Li, B.; Shao, H.; Li, W.; Lin, H. Catalysis and downsizing in Mg-Based hydrogen storage materials. *Catalysts* **2018**, *8*, 89. [CrossRef]
16. Li, B.; Li, J.; Shao, H.; He, L. Mg-based hydrogen absorbing materials for thermal energy storage—A Review. *Appl. Sci.* **2018**, *8*, 1375. [CrossRef]
17. Shao, H.; Xin, G.; Zheng, J.; Li, X.; Akiba, E. Nanotechnology in Mg-based materials for hydrogen storage. *Nano Energy* **2012**, *1*, 590–601. [CrossRef]
18. Zaluska, A.; Zaluski, L.; Ström–Olsen, J.O. Nanocrystalline magnesium for hydrogen storage. *J. Alloy. Compd.* **1999**, *288*, 217–225. [CrossRef]

19. Huot, J.; Liang, G.; Boily, S.; Van Neste, A.; Schulz, R. Structural study and hydrogen sorption kinetics of ball-milled magnesium hydride. *J. Alloy. Compd.* **1999**, *293*, 495–500. [CrossRef]
20. Jerkiewicz, G. Hydrogen sorption ATIN electrodes. *Prog. Surf. Sci.* **1998**, *57*, 137–186. [CrossRef]
21. Züttel, A.; Güther, V.; Otto, A.; Bartsch, M.; Kotz, R.; Chartouni, D.; Nutzenadel, C.; Schlapbach, L. About the mechanism and the rate limiting step of the metalhydride electrode reaction. *J. Alloy. Compd.* **1999**, *293–295*, 663–669. [CrossRef]
22. Tliha, M.; Mathlouthi, H.; Lamloumi, J.; Percheron-Guegan, A. AB5-type hydrogen storage alloy used as anodic materials in Ni-MH batteries. *J. Alloy. Compd.* **2007**, *436*, 221–225. [CrossRef]
23. Cui, N.; Luo, J.L.; Chuang, K.T. Nickel–metal hydride (Ni-MH) battery using Mg_2Ni-type hydrogen storage alloy. *J. Alloy. Compd.* **2000**, *302*, 218–226. [CrossRef]
24. Xiong, W.; Yan, H.; Wang, L.; Verbetsky, V.; Zhao, X.; Mitrokhin, S.; Li, B.; Li, J.; Wang, Y. Characteristics of A_2B_7-type LaYNi-based hydrogen storage alloys modified by partially substituting Ni with Mn. *Int. J. Hydrogen Energy* **2017**, *42*, 10131–10141. [CrossRef]
25. Wang, C.; Soriaga, M.P.; Srinivasan, S. Determination of reaction resistances for metal-hydride electrodes during anodic polarization. *J. Power Sources* **2000**, *85*, 212–223. [CrossRef]
26. Zhang, H.; Zheng, X.; Tian, X.; Liu, Y.; Li, X. New approaches for rare earth-magnesium based hydrogen storage alloys. *Prog. Nat. Sci. Mater. Int.* **2017**, *27*, 50–57. [CrossRef]
27. Wei, T.Y.; Lim, K.L.; Tseng, Y.S.; Chan, S.L.I. A review on the characterization of hydrogen in hydrogen storage materials. *Renew. Sustain. Energy Rev.* **2017**, *79*, 1122–1133. [CrossRef]
28. Wang, Y.; Tang, W.; Wang, F.; Ding, C.; Xu, S.; Yu, R. Effects of surface coating with Cu–Pd on electrochemical properties of A_2B_7-type hydrogen storage alloy. *Int. J. Hydrogen Energy* **2018**, *43*, 3244–3252. [CrossRef]
29. Shen, W.; Han, S.; Li, Y.; Yang, J.; Xiao, K. Electrochemical performance of polyaniline electroless deposited La–Mg–Ni-based hydrogen storage alloys. *Mater. Chem. Phys.* **2012**, *132*, 852–857. [CrossRef]
30. House, S.D.; Vajo, J.J.; Ren, C.; Rockett, A.A.; Robertson, I.M. Effect of ball-milling duration and dehydrogenation on the morphology, microstructure and catalyst dispersion in Ni-catalyzed MgH_2 hydrogen storage materials. *Acta Mater.* **2015**, *86*, 55–68. [CrossRef]
31. Ouyang, L.Z.; Cao, Z.J.; Li, L.L.; Wang, H.; Liu, J.W.; Min, D.; Chen, Y.W.; Xiao, F.M.; Tang, R.H.; Zhu, M. Enhanced high-rate discharge properties of $La_{11.3}Mg_{6.0}Sm_{7.4}Ni_{61.0}$ $Co_{7.2}Al_{7.1}$ with added graphene synthesized by plasma milling. *Int. J. Hydrogen Energy* **2014**, *39*, 12765–12772. [CrossRef]
32. Zhang, Z.; Jin, J.; Zhang, H.; Qi, X.; Bian, Y.; Zhao, H. First-principles calculation of hydrogen adsorption and diffusion on Mn-doped Mg_2Ni (010) surfaces. *Appl. Surf. Sci.* **2017**, *425*, 148–155. [CrossRef]
33. Li, Q.; Lu, Y.; Luo, Q.; Yang, X.; Yang, Y.; Tan, J.; Dong, Z.; Dang, J.; Li, J.; Chen, Y.; et al. Thermodynamics and kinetics of hydriding and dehydriding reactions in Mg-based hydrogen storage materials. *J. Magnes. Alloy.* **2021**, *9*, 1922–1941. [CrossRef]
34. Züttel, A. Materials for hydrogen storage. *Mater. Today* **2003**, *6*, 24–33. [CrossRef]
35. Banerjee, S.; Pillai, C.G.S.; Majumder, C. Dissociation and diffusion of hydrogen on the Mg (0001) surface: Catalytic effect of V and Ni double substitution. *J. Phys. Chem. C* **2009**, *113*, 10574–10579. [CrossRef]
36. Martino, P.; Chiesa, M.; Cristina Paganini, M.; Giamello, E. Coadsorption of NO and H_2 at the surface of MgO monitored by EPR spectroscopy. Towards a site specific discrimination of polycrystalline oxide surfaces. *Surf. Sci.* **2003**, *527*, 80–88. [CrossRef]
37. Liu, Y.; Cao, Y.; Huang, L.; Gao, M.; Pan, H. Rare earth–Mg–Ni-based hydrogen storage alloys as negative electrode materials for Ni/MH batteries. *J. Alloy. Compd.* **2011**, *509*, 675–686. [CrossRef]
38. Feng, F.; Geng, M.; Northwood, D.O. Electrochemical behaviour of intermetallic-based metal hydrides used in Ni/metal hydride (MH) batteries: A review. *Int. J. Hydrogen Energy* **2001**, *26*, 725–734. [CrossRef]
39. Zhao, X.; Ding, Y.; Ma, L.; Wang, L.; Yang, M.; Shen, X. Electrochemical properties of $MmNi_{3.8}Co_{0.75}Mn_{0.4}Al_{0.2}$ hydrogen storage alloy modified with nanocrystalline nickel. *Int. J. Hydrogen Energy* **2008**, *33*, 6727–6733. [CrossRef]
40. Zhu, Y.; Yang, C.; Zhu, J.; Li, L. Structural and electrochemical hydrogen storage properties of Mg_2Ni-based alloys. *J. Alloy. Compd.* **2011**, *509*, 5309–5314. [CrossRef]
41. Zhu, M.; Lu, Y.; Ouyang, L.; Wang, H. Thermodynamic tuning of Mg-based hydrogen storage alloys: A Review. *Materials* **2013**, *6*, 4654–4674. [CrossRef] [PubMed]
42. Luo, Q.; Li, J.; Li, B.; Liu, B.; Shao, H.; Li, Q. Kinetics in Mg-based hydrogen storage materials: Enhancement and mechanism. *J. Magnes. Alloy.* **2019**, *7*, 58–71. [CrossRef]
43. Arboleda, J.N.B.; Kasai, H.; Nobuhara, K.; Diño, W.A.; Nakanishi, H. Dissociation and Sticking of H_2 on Mg(0001), Ti(0001) and La(0001) Surfaces. *J. Phys. Soc. Jpn.* **2004**, *73*, 745–748. [CrossRef]
44. Bérubé, V.; Radtke, G.; Dresselhaus, M.; Chen, G. Size effects on the hydrogen storage properties of nanostructured metal hydrides: A review. *Int. J. Energy Res.* **2007**, *31*, 637–663. [CrossRef]
45. Sakintuna, B.; Lamaridarkrim, F.; Hirscher, M. Metal hydride materials for solid hydrogen storage: A review. *Int. J. Hydrogen Energy* **2007**, *32*, 1121–1140. [CrossRef]
46. Aguey-Zinsou, K.F.; Ares-Fernández, J.R. Hydrogen in magnesium: New perspectives toward functional stores. *Energy Environ. Sci.* **2010**, *3*, 526–543. [CrossRef]
47. Floriano, R.; Deledda, S.; Hauback, B.C.; Leiva, D.R.; Botta, W.J. Iron and niobium based additives in magnesium hydride: Microstructure and hydrogen storage properties. *Int. J. Hydrogen Energy* **2017**, *42*, 6810–6819. [CrossRef]

48. Mirabile Gattia, D.; Jangir, M.; Jain, I.P. Study on nanostructured MgH_2 with Fe and its oxides for hydrogen storage applications. *J. Alloy. Compd.* **2019**, *801*, 188–191. [CrossRef]
49. Aurora, A.; Mancini, M.R.; Gattia, D.M.; Montone, A.; Pilloni, L.; Todini, E.; Antisari, M.V. Microstructural and kinetic investigation of hydrogen sorption reaction of MgH_2/Nb_2O_5 nanopowders. *Mater. Manuf. Process.* **2009**, *24*, 1058–1063. [CrossRef]
50. Crivello, J.C.; Dam, B.; Denys, R.V.; Dornheim, M.; Grant, D.M.; Huot, J.; Jensen, T.R.; de Jongh, P.; Latroche, M.; Milanese, C.; et al. Review of magnesium hydride-based materials: Development and optimisation. *Appl. Phys. A.* **2016**, *122*, 1–20. [CrossRef]
51. Yu, H.; Bennici, S.; Auroux, A. Hydrogen storage and release: Kinetic and thermodynamic studies of MgH_2 activated by transition metal nanoparticles. *Int. J. Hydrogen Energy* **2014**, *39*, 11633–11641. [CrossRef]
52. Barkhordarian, G.; Klassen, T.; Bormann, R. Fast hydrogen sorption kinetics of nanocrystalline Mg using Nb_2O_5 as catalyst. *Scr. Mater.* **2003**, *49*, 213–217. [CrossRef]
53. Özkar, S.; Finke, R.G. Nanocluster formation and stabilization fundamental studies: Ranking commonly employed anionic stabilizers via the development, then application, of five comparative criteria. *J. Am. Chem. Soc.* **2002**, *124*, 5796–5810. [CrossRef] [PubMed]
54. Tang, Q.; Zhang, Q.; Wang, P.; Wang, Y.; Wan, H. Characterizations of cobalt oxide nanoparticles within faujasite zeolites and the formation of metallic cobalt. *Chem. Mater.* **2004**, *16*, 1967–1976. [CrossRef]
55. Aiken III, J.D.; Finke, R.G. A review of modern transition-metal nanoclusters: Their synthesis, characterization, and applications in catalysis. *J. Mol. Catal. A Chem.* **1999**, *145*, 1–44. [CrossRef]
56. Özkar, S. Enhancement of catalytic activity by increasing surface area in heterogeneous catalysis. *Appl. Surf. Sci.* **2009**, *256*, 1272–1277. [CrossRef]
57. Gross, A.F.; Ahn, C.C.; Van Atta, S.L.; Liu, P.; Vajo, J.J. Fabrication and hydrogen sorption behaviour of nanoparticulate MgH_2 incorporated in a porous carbon host. *Nanotechnology* **2009**, *20*, 204005. [CrossRef]
58. Paskevicius, M.; Tian, H.-Y.; Sheppard, D.A.; Webb, C.J.; Pitt, M.P.; Gray, E.M.; Kirby, N.M.; Buckley, C.E. Magnesium hydride formation within carbon aerogel. *J. Phys. Chem. C* **2011**, *115*, 1757–1766. [CrossRef]
59. Adelhelm, P.; de Jongh, P.E. The impact of carbon materials on the hydrogen storage properties of light metal hydrides. *J. Mater. Chem.* **2011**, *21*, 2417–2427. [CrossRef]
60. Korkmaz, S.; Kariper, İ.A. Graphene and graphene oxide based aerogels: Synthesis, characteristics and supercapacitor applications. *J. Energy Storage* **2020**, *27*, 101038. [CrossRef]
61. Liu, G.; Wang, Y.; Qiu, F.; Li, L.; Jiao, L.; Yuan, H. Synthesis of porous Ni@rGO nanocomposite and its synergetic effect on hydrogen sorption properties of MgH_2. *J. Mater. Chem.* **2012**, *22*, 22542. [CrossRef]
62. Liu, M.; Xiao, X.; Zhao, S.; Saremi-Yarahmadi, S.; Chen, M.; Zheng, J.; Li, S.; Chen, L. ZIF-67 derived Co@CNTs nanoparticles: Remarkably improved hydrogen storage properties of MgH_2 and synergetic catalysis mechanism. *Int. J. Hydrogen Energy* **2019**, *44*, 1059–1069. [CrossRef]
63. Hudson, M.S.L.; Takahashi, K.; Ramesh, A.; Awasthi, S.; Ghosh, A.K.; Ravindran, P.; Srivastava, O.N. Graphene decorated with Fe nanoclusters for improving the hydrogen sorption kinetics of MgH_2-experimental and theoretical evidence. *Catal. Sci. Technol.* **2016**, *6*, 261–268. [CrossRef]
64. Bhatnagar, A.; Pandey, S.K.; Vishwakarma, A.K.; Singh, S.; Shukla, V.; Soni, P.K.; Shaz, M.A.; Srivastava, O.N. Fe_3O_4@graphene as a superior catalyst for hydrogen de/absorption from/in MgH_2/Mg. *J. Mater. Chem. A* **2016**, *4*, 14761–14772. [CrossRef]
65. Xie, X.; Chen, M.; Liu, P.; Shang, J.; Liu, T. High hydrogen desorption properties of Mg-based nanocomposite at moderate temperatures: The effects of multiple catalysts in situ formed by adding nickel sulfides/graphene. *J. Power Sources* **2017**, *371*, 112–118. [CrossRef]
66. Wang, S.; Gao, M.; Yao, Z.; Xian, K.; Wu, M.; Liu, Y.; Sun, W.; Pan, H. High-loading, ultrafine Ni nanoparticles dispersed on porous hollow carbon nanospheres for fast (de)hydrogenation kinetics of MgH_2. *J. Magnes. Alloy.* **2022**, *10*, 3354–3366. [CrossRef]
67. Ma, Z.; Tang, Q.; Ni, J.; Zhu, Y.; Zhang, Y.; Li, H.-W.; Zhang, J.; Liu, Y.; Ba, Z.; Li, L. Synergistic effect of TiH_2 and air exposure on enhancing hydrogen storage performance of Mg_2NiH_4. *Chem. Eng. J.* **2022**, *433*, 134489. [CrossRef]
68. Wang, L.; Quadir, M.Z.; Aguey-Zinsou, K.-F. Ni coated LiH nanoparticles for reversible hydrogen storage. *Int. J. Hydrogen Energy* **2016**, *41*, 6376–6386. [CrossRef]
69. Sun, Y.; Shen, C.; Lai, Q.; Liu, W.; Wang, D.-W.; Aguey-Zinsou, K.-F. Tailoring magnesium based materials for hydrogen storage through synthesis: Current state of the art. *Energy Storage Mater.* **2018**, *10*, 168–198. [CrossRef]
70. Norberg, N.S.; Arthur, T.S.; Fredrick, S.J.; Prieto, A.L. Size-dependent hydrogen storage properties of Mg nanocrystals prepared from solution. *J. Am. Chem. Soc.* **2011**, *133*, 10679–10681. [CrossRef]
71. Zaluski, L.; Zaluska, A.; Ström-Olsen, J.O. Hydrogen absorption in nanocrystalline Mg_2Ni formed by mechanical alloying. *J. Alloy. Compd.* **1995**, *217*, 245–249. [CrossRef]
72. Shao, H.; Asano, K.; Enoki, H.; Akiba, E. Fabrication, hydrogen storage properties and mechanistic study of nanostructured $Mg_{50}Co_{50}$ body-centered cubic alloy. *Scr. Mater.* **2009**, *60*, 818–821. [CrossRef]
73. Shao, H.; Matsuda, J.; Li, H.-W.; Akiba, E.; Jain, A.; Ichikawa, T.; Kojima, Y. Phase and morphology evolution study of ball milled Mg–Co hydrogen storage alloys. *Int. J. Hydrogen Energy* **2013**, *38*, 7070–7076. [CrossRef]
74. Zhang, Y.; Wei, X.; Zhang, W.; Yuan, Z.; Gao, J.; Qi, Y.; Ren, H. Effect of milling duration on hydrogen storage thermodynamics and kinetics of Mg-based alloy. *Int. J. Hydrogen Energy* **2020**, *45*, 33832–33845. [CrossRef]

75. Chen, J.; Takeshita, H.T.; Chartouni, D.; Kuriyama, N.; Sakai, T. Synthesis and characterization of nanocrystalline Mg_2CoH_5 obtained by mechanical alloying. *J. Mater. Sci.* **2001**, *36*, 5829–5834. [CrossRef]
76. Herrich, M.; Ismail, N.; Lyubina, J.; Handstein, A.; Pratt, A.; Gutfleisch, O. Synthesis and decomposition of Mg_2FeH_6 prepared by reactive milling. *Mater. Sci. Eng. B* **2004**, *108*, 28–32. [CrossRef]
77. Li, W.; Li, C.; Ma, H.; Chen, J. Magnesium nanowires: Enhanced kinetics for hydrogen absorption and desorption. *J. Am. Chem. Soc.* **2007**, *129*, 6710–6711. [CrossRef]
78. Venturi, F.; Calizzi, M.; Bals, S.; Perkisas, T.; Pasquini, L. Self-assembly of gas-phase synthesized magnesium nanoparticles on room temperature substrates. *Mater. Res. Express* **2014**, *2*, 2015007. [CrossRef]
79. Choi, Y.J.; Choi, J.W.; Sohn, H.Y.; Ryu, T.; Hwang, K.S.; Fang, Z.Z. Chemical vapor synthesis of Mg–Ti nanopowder mixture as a hydrogen storage material. *Int. J. Hydrogen Energy* **2009**, *34*, 7700–7706. [CrossRef]
80. Nielsen, T.K.; Manickam, K.; Hirscher, M.; Besenbacher, F.; Jensen, T.R. Confinement of MgH_2 nanoclusters within nanoporous aerogel scaffold materials. *ACS Nano* **2009**, *3*, 3521–3528. [CrossRef]
81. Au, Y.S.; Obbink, M.K.; Srinivasan, S.; Magusin, P.C.M.M.; de Jong, K.P.; de Jongh, P.E. The size dependence of hydrogen mobility and sorption kinetics for carbon-supported MgH_2 particles. *Adv. Funct. Mater.* **2014**, *24*, 3604–3611. [CrossRef]
82. Zlotea, C.; Chevalier-Cesar, C.; Leonel, E.; Leroy, E.; Cuevas, F.; Dibandjo, P.; Vix-Guterl, C.; Martens, T.; Latroche, M. Synthesis of small metallic Mg-based nanoparticles confined in porous carbon materials for hydrogen sorption. *Faraday Discuss* **2011**, *151*, 117–131. [CrossRef] [PubMed]
83. Zhang, S.; Gross, A.F.; Van Atta, S.L.; Lopez, M.; Liu, P.; Ahn, C.C.; Vajo, J.J.; Jensen, C.M. The synthesis and hydrogen storage properties of a MgH_2 incorporated carbon aerogel scaffold. *Nanotechnology* **2009**, *20*, 204027. [CrossRef] [PubMed]
84. Zlotea, C.; Oumellal, Y.; Hwang, S.-J.; Ghimbeu, C.M.; de Jongh, P.E.; Latroche, M. Ultrasmall MgH_2 nanoparticles embedded in an ordered microporous carbon exhibiting rapid hydrogen sorption kinetics. *J. Phys. Chem. C* **2015**, *119*, 18091–18098. [CrossRef]
85. Chen, M.; Hu, M.; Xie, X.; Liu, T. High loading nanoconfinement of V–decorated Mg with 1 nm carbon shells: Hydrogen storage properties and catalytic mechanism. *Nanoscale* **2019**, *11*, 10045–10055. [CrossRef]
86. Jia, Y.; Sun, C.; Cheng, L.; Wahab, M.A.; Cui, J.; Zou, J.; Zhu, M.; Yao, X. Destabilization of Mg-H bonding through nano-interfacial confinement by unsaturated carbon for hydrogen desorption from MgH_2. *Phys. Chem. Chem. Phys.* **2013**, *15*, 5814–5820. [CrossRef]
87. Johnson, N.J.J.; Lam, B.; MacLeod, B.P.; Sherbo, R.S.; Moreno-Gonzalez, M.; Fork, D.K.; Berlinguette, C.P. Facets and vertices regulate hydrogen uptake and release in palladium nanocrystals. *Nat. Mater.* **2019**, *18*, 454–458. [CrossRef]
88. Ye, J.-H.; Zhao, Y.-J.; Fang, Y.-X.; Lin, H.-J.; Bai, L.; Tang, J.-J. Hydrogen adsorption, dissociation, and diffusion on high-index Mg(1013) and their comparisons with Mg(0001): A systematic first-principles study. *Int. J. Hydrogen Energy* **2019**, *44*, 4897–4906. [CrossRef]
89. Dun, C.; Jeong, S.; Kwon, D.-H.; Kang, S.; Stavila, V.; Zhang, Z.; Lee, J.-W.; Mattox, T.M.; Heo, T.W.; Wood, B.C.; et al. Hydrogen storage performance of preferentially oriented Mg/rGO hybrids. *Chem. Mater.* **2022**, *34*, 2963–2971. [CrossRef]
90. Kim, K.C.; Dai, B.; Johnson, J.K.; Sholl, D.S. Assessing nanoparticle size effects on metal hydride thermodynamics using the Wulff construction. *Nanotechnology* **2009**, *20*, 204001. [CrossRef]
91. Vajeeston, P.; Ravindran, P.; Fichtner, M.; Fjellvåg, H. Influence of crystal structure of bulk phase on the stability of nanoscale phases: Investigation on MgH_2 derived nanostructures. *J. Phys. Chem. C* **2012**, *116*, 18965–18972. [CrossRef]
92. Vajeeston, P.; Sartori, S.; Ravindran, P.; Knudsen, K.D.; Hauback, B.; Fjellvåg, H. MgH_2 in carbon scaffolds: A combined experimental and theoretical investigation. *J. Phys. Chem. C* **2012**, *116*, 21139–21147. [CrossRef]
93. Liu, W.; Aguey-Zinsou, K.F. Size effects and hydrogen storage properties of Mg nanoparticles synthesised by an electroless reduction method. *J. Mater. Chem. A* **2014**, *2*, 9718–9726. [CrossRef]
94. Liu, M.; Xiao, X.; Zhao, S.; Chen, M.; Mao, J.; Luo, B.; Chen, L. Facile synthesis of Co/Pd supported by few-walled carbon nanotubes as an efficient bidirectional catalyst for improving the low temperature hydrogen storage properties of magnesium hydride. *J. Mater. Chem. A* **2019**, *7*, 5277–5287. [CrossRef]
95. Lotoskyy, M.; Denys, R.; Yartys, V.A.; Eriksen, J.; Goh, J.; Nyamsi, S.N.; Sita, C.; Cummings, F. An outstanding effect of graphite in nano-MgH_2–TiH_2 on hydrogen storage performance. *J. Mater. Chem. A* **2018**, *6*, 10740–10754. [CrossRef]
96. Cui, J.; Wang, H.; Liu, J.; Ouyang, L.; Zhang, Q.; Sun, D.; Yao, X.; Zhu, M. Remarkable enhancement in dehydrogenation of MgH_2 by a nano-coating of multi-valence Ti-based catalysts. *J. Mater. Chem. A* **2013**, *1*, 5603–5611. [CrossRef]
97. Cui, J.; Liu, J.; Wang, H.; Ouyang, L.; Sun, D.; Zhu, M.; Yao, X. Mg–TM (TM: Ti, Nb, V, Co, Mo or Ni) core–shell like nanostructures: Synthesis, hydrogen storage performance and catalytic mechanism. *J. Mater. Chem. A* **2014**, *2*, 9645–9655. [CrossRef]
98. Zou, J.; Zeng, X.; Ying, Y.; Chen, X.; Guo, H.; Zhou, S.; Ding, W. Study on the hydrogen storage properties of core-shell structured Mg–RE (RE = Nd, Gd, Er) nano-composites synthesized through arc plasma method. *Int. J. Hydrogen Energy* **2013**, *38*, 2337–2346. [CrossRef]
99. Mao, J.; Zou, J.; Lu, C.; Zeng, X.; Ding, W. Hydrogen storage and hydrolysis properties of core-shell structured Mg-MF_x (M=V, Ni, La and Ce) nano-composites prepared by arc plasma method. *J. Power Sources* **2017**, *366*, 131–142. [CrossRef]
100. Jain, I.P. Hydrogen the fuel for 21st century. *Int. J. Hydrogen Energy* **2009**, *34*, 7368–7378. [CrossRef]
101. Zou, J.; Guo, H.; Zeng, X.; Zhou, S.; Chen, X.; Ding, W. Hydrogen storage properties of Mg–TM–La (TM = Ti, Fe, Ni) ternary composite powders prepared through arc plasma method. *Int. J. Hydrogen Energy* **2013**, *38*, 8852–8862. [CrossRef]

102. Lu, C.; Zou, J.; Shi, X.; Zeng, X.; Ding, W. Synthesis and hydrogen storage properties of core-shell structured binary Mg@Ti and ternary Mg@Ti@Ni composites. *Int. J. Hydrogen Energy* **2017**, *42*, 2239–2247. [CrossRef]
103. Lu, C.; Zou, J.; Zeng, X.; Ding, W. Hydrogen storage properties of core-shell structured Mg@TM (TM=Co, V) composites. *Int. J. Hydrogen Energy* **2017**, *42*, 15246–15255. [CrossRef]
104. Jeon, K.J.; Moon, H.R.; Ruminski, A.M.; Jiang, B.; Kisielowski, C.; Bardhan, R.; Urban, J.J. Air-stable magnesium nanocomposites provide rapid and high-capacity hydrogen storage without using heavy-metal catalysts. *Nat. Mater.* **2011**, *10*, 286–290. [CrossRef]
105. Xia, G.; Tan, Y.; Chen, X.; Sun, D.; Guo, Z.; Liu, H.; Ouyang, L.; Zhu, M.; Yu, X. Monodisperse magnesium hydride nanoparticles uniformly self-assembled on graphene. *Adv. Mater.* **2015**, *27*, 5981–5988. [CrossRef]
106. Callini, E.; Pasquini, L.; Piscopiello, E.; Montone, A.; Vittori Antisari, M.; Bonetti, E. Hydrogen sorption in Pd-decorated Mg–MgO core-shell nanoparticles. *Appl. Phys. Lett.* **2009**, *94*, 221905. [CrossRef]
107. Ma, Z.; Panda, S.; Zhang, Q.; Sun, F.; Khan, D.; Ding, W.; Zou, J. Improving hydrogen sorption performances of MgH_2 through nanoconfinement in a mesoporous CoS nano-boxes scaffold. *Chem. Eng. J.* **2021**, *406*, 126790. [CrossRef]
108. Wang, W.; Liu, X.; Zhang, L.; Zhang, S.; Guo, W.; Zhao, Y.; Zhang, H.; Li, Y.; Han, S. The electrochemical characteristics of AB_4-type rare earth-Mg–Ni-based superlattice structure hydrogen storage alloys for nickel metal hydride battery. *J. Magnes. Alloy.* **2021**, *9*, 2039–2048. [CrossRef]
109. Ouyang, L.; Huang, J.; Wang, H.; Liu, J.; Zhu, M. Progress of hydrogen storage alloys for Ni-MH rechargeable power batteries in electric vehicles: A review. *Mater. Chem. Phys.* **2017**, *200*, 164–178. [CrossRef]
110. Liu, Y.; Pan, H.; Gao, M.; Wang, Q. Advanced hydrogen storage alloys for Ni/MH rechargeable batteries. *J. Mater. Chem.* **2011**, *21*, 4743–4755. [CrossRef]
111. Young, K.H.; Nei, J. The current status of hydrogen storage alloy development for electrochemical applications. *Materials* **2013**, *6*, 4574–4608. [CrossRef] [PubMed]
112. Kleperis, J.; Wojcik, G.; Czerwinski, A.; Skowronski, J.; Kopczyk, M.; Beltowska-Brzezinska, M. Electrochemical behavior of metal hydrides. *J. Solid State Electrochem.* **2001**, *5*, 229–249. [CrossRef]
113. Cuevas, F.; Joubert, J.M.; Latroche, M.; Percheron-Guégan, A. Intermetallic compounds as negative electrodes of Ni/MH batteries. *Appl. Phys. A Mater. Sci. Process.* **2001**, *72*, 225–238. [CrossRef]
114. Sünbül, S.E.; Öztürk, S.; İçin, K. Structural and hydrogen storage properties of Mg_{60}-Ni_{40} and Mg_{80}-Ni_{20} alloys prepared by planar flow casting. *J. Mater. Eng. Perform.* **2020**, *29*, 6101–6107. [CrossRef]
115. Charbonnier, V.; Madern, N.; Monnier, J.; Zhang, J.; Paul-Boncour, V.; Latroche, M. Relationship between H_2 sorption, electrochemical cycling and aqueous corrosion properties in A_5Ni_{19} hydride-forming alloys (A = Gd, Sm). *J. Power Sources* **2018**, *397*, 280–287. [CrossRef]
116. Wang, C.C.; Zhou, Y.T.; Yang, C.C.; Jiang, Q. A strategy for designing new $AB_{4.5}$-type hydrogen storage alloys with high capacity and long cycling life. *J. Power Sources* **2018**, *398*, 42–48. [CrossRef]
117. Zhao, X.; Ma, L. Recent progress in hydrogen storage alloys for nickel/metal hydride secondary batteries. *Int. J. Hydrogen Energy* **2009**, *34*, 4788–4796. [CrossRef]
118. Jia, Z.; Zhang, L.; Zhao, Y.; Cao, J.; Li, Y.; Dong, Z.; Wang, W.; Han, S. Self-discharge characteristic and mechanism of single-phase $PuNi_3$-, Gd_2Co_7-, and Pr_5Co_{19}-type Nd–Mg–Ni-based alloys. *J. Power Sources* **2017**, *371*, 188–196. [CrossRef]
119. Cui, N.; Luan, B.; Liu, H.K.; Dou, S.X. Discharge behaviour of Mg_2Ni-typehydrogen-storage alloy electrodes in 6 M KOH solution by electrochemical impedance spectroscopy. *J. Power Sources* **1996**, *63*, 209–214. [CrossRef]
120. Li, M.M.; Yang, C.C.; Wang, C.C.; Wen, Z.; Zhu, Y.F.; Zhao, M.; Li, J.C.; Zheng, W.T.; Lian, J.S.; Jiang, Q. Design of hydrogen storage alloys/nanoporous metals hybrid electrodes for nickel-metal hydride batteries. *Sci. Rep.* **2016**, *6*, 27601. [CrossRef]
121. Giza, K.; Drulis, H. Effect of preparation method of metal hydride electrode on efficiency of hydrogen electrosorption process. *Int. J. Mater. Res.* **2016**, *107*, 103–108. [CrossRef]
122. Wang, F.; Li, R.; Ding, C.; Wan, J.; Yu, R.; Wang, Z. Effect of catalytic Ni coating with different depositing time on the hydrogen storage properties of ZrCo alloy. *Int. J. Hydrogen Energy* **2016**, *41*, 17421–17432. [CrossRef]
123. Sakai, T.; Yuasa, A.; Ishikawa, H.; Miyamura, H.; Kuriyama, N. Nickel-metal hydride battery using microencapsulated alloys. *J. Less Common Met.* **1991**, *172–174*, 1194–1204. [CrossRef]
124. Sakai, T.; Miyamura, H.; Kuriyama, N.; Ishikawa, H.; Uehara, I. Hydrogen storage alloys for nickel-metal hydride battery. *Z. Für Phys. Chemie.* **1994**, *183*, 333–346. [CrossRef]
125. Sun, L.; Lin, J.; Liang, F.; Cao, Z.; Wang, L. Ni coated $Ti_{1.4}V_{0.6}Ni$ composite as the negative electrode in Ni-MH battery. *Mater. Letters.* **2015**, *161*, 686–689. [CrossRef]
126. Li, M.M.; Yang, C.C.; Chen, L.X.; Jiang, Q. Hydrogen storage alloys/reduced graphite oxide: An efficient hybrid electrode with enhanced high-rate dischargeability. *Electrochim. Acta.* **2016**, *200*, 59–65. [CrossRef]
127. Zadorozhnyy, M.Y.; Klyamkin, S.N.; Strugova, D.V.; Olifirov, L.K.; Milovzorov, G.S.; Kaloshkin, S.D.; Zadorozhnyy, V.Y. Deposition of polymer coating on metallic powder through ball milling: Application to hydrogen storage intermetallics. *Int. J. Energy Res.* **2016**, *40*, 273–279. [CrossRef]
128. Chen, W.; Zhu, Y.; Yang, C.; Zhang, J.; Li, M.; Li, L. Significantly improved electrochemical hydrogen storage properties of magnesium nickel hydride modified with nano-nickel. *J. Power Sources* **2015**, *280*, 132–140. [CrossRef]

129. Wang, B.; Zhao, L.; Cai, C.; Wang, S. Effects of surface coating with polyaniline on electrochemical properties of La-Mg-Ni-based electrode alloys. *Int. J. Hydrogen Energy* **2014**, *39*, 10374–10379. [CrossRef]
130. Huang, L.; Wang, Y.; Huang, Z.; Tang, J.; Wang, Y.; Liu, J.; Jiao, J.; Liu, J.; Belfiore, L.A. Effects of graphene/silver nanohybrid additives on electrochemical properties of magnesium-based amorphous alloy. *J. Power Sources* **2014**, *269*, 716–722. [CrossRef]
131. Li, Y.; Wang, C.; Dong, Z.; Wang, J.; Yang, S.; Ke, D.; Han, S. Effects of coating layers on electrochemical properties of Nd–Mg–Ni-based alloys. *Int. J. Hydrogen Energy* **2017**, *42*, 19148–19155. [CrossRef]
132. Du, Y.; Li, N.; Zhang, T.L.; Feng, Q.P.; Du, Q.; Wu, X.H.; Huang, G.W. Reduced graphene oxide coating with anticorrosion and electrochemical property-enhancing effects applied in hydrogen storage system. *ACS Appl. Mater. Interfaces* **2017**, *9*, 28980–28989. [CrossRef] [PubMed]
133. Yang, S.; Liu, H.; Han, S.; Li, Y.; Shen, W. Effects of electroless composite plating Ni–Cu–P on the electrochemical properties of La-Mg-Ni-based hydrogen storage alloy. *Appl. Surf. Sci.* **2013**, *271*, 210–215. [CrossRef]
134. Zhang, H.; Fu, L.; Xuan, W.; Li, X. Nano-Ni induced surface modification relevant to the hydrogenation performances in La–Mg based alloys. *Appl. Surf. Sci.* **2018**, *439*, 18–23. [CrossRef]
135. Zhang, H.; Fu, L.; Xuan, W.; Qin, H.; Ji, Z. Ni–Al films induced surface modification of La_2Mg_{17} alloy leading to improved dehydrogenation properties. *J. Power Sources* **2018**, *385*, 27–31. [CrossRef]
136. Santos, S.F.; de Castro, J.F.R.; Ishikawa, T.T.; Ticianelli, E.A. Effect of mechanical coating with Ni and Ni-5% Al on the structure and electrochemical properties of the Mg-50% Ni alloy. *J. Mater. Sci.* **2008**, *43*, 2889–2894. [CrossRef]
137. Ranjbar, A.; Aminorroaya, S.; Guo, Z.P.; Cho, Y.; Liu, H.K.; Dahle, A. Comparison of hydrogen storage properties of Mg–Ni from different preparation methods. *Mater. Chem. Phys.* **2011**, *127*, 405–408. [CrossRef]
138. Guzmán, D.; Ordoñez, S.; Fernández, J.F.; Sánchez, C.; Serafini, D.; Rojas, P.A.; Aguilar, C.; Tapia, P. Effect of amorphous $Mg_{50}Ni_{50}$ on hydriding and dehydriding behavior of Mg_2Ni alloy. *Mater. Charact.* **2011**, *62*, 442–450. [CrossRef]
139. Tian, Q.; Zhang, Y.; Sun, L.; Xu, F.; Tan, Z.; Yuan, H.; Zhang, T. Effects of Pd substitution on the electrochemical properties of $Mg_{0.9-x}Ti_{0.1}Pd_xNi$ (x = 0.04–0.1) hydrogen storage alloys. *J. Power Sources* **2006**, *158*, 1463–1471. [CrossRef]
140. Zhang, Y.; Gao, J.; Yuan, Z.; Wei, X.; Zhang, W.; Qi, Y.; Zhao, D. Effect of graphite (GR) content on electrochemical hydrogen storage performances of nanocrystalline and amorphous $La_9Ce_1Mg_{80}Ni_5$–Ni–GR composites synthesized by mechanical milling. *Int. J. Hydrogen Energy* **2020**, *45*, 29023–29033. [CrossRef]
141. Zhang, Y.; Wang, G.; Dong, X.; Guo, S.; Ren, J.; Wang, X. Effect of substituting Co with Fe on the cycle stabilities of the as-cast and quenched AB5-type hydrogen storage alloys. *J. Power Sources* **2005**, *148*, 105–111. [CrossRef]
142. Zhang, Y.; Li, B.; Ren, H.; Cai, Y.; Dong, X.; Wang, X. Cycle stabilities of the $La_{0.7}Mg_{0.3}Ni_{2.55-x}Co_{0.45}M_x$ (M=Fe, Mn, Al; x=0, 0.1) electrode alloys prepared by casting and rapid quenching. *J. Alloy. Compd.* **2008**, *458*, 340–345. [CrossRef]
143. Yong, H.; Wei, X.; Wang, Y.; Guo, S.; Yuan, Z.; Qi, Y.; Zhao, D.; Zhang, Y. Phase evolution, thermodynamics and kinetics property of transition metal (TM = Zr, Ti, V) catalyzed Mg–Ce–Y–Ni hydrogen storage alloys. *J. Phys. Chem. Solids* **2020**, *144*, 109516. [CrossRef]
144. Bu, W.; Peng, W.; Liu, Q.; Li, L.; Li, W.; Dai, X. Nanocrystalline structure and electrochemical hydrogen storage properties of the as-milled Mg–V–Ni–Fe–Zn-based materials. *Int. J. Hydrogen Energy* **2023**, *48*, 6937–6946. [CrossRef]
145. Gan, H.; Yang, Y.; Shao, H. Improvement of the rate performance of hydrogen storage alloys by heat treatments in Ar and H_2/Ar atmosphere for high-power nickel–metal hydride batteries. *Electrochim. Acta* **2015**, *174*, 164–171. [CrossRef]
146. Ji, Z.; Wang, Z.; Deng, J.; Yao, Q.; Zhou, H. Effects of surface treatment on electrochemical properties of $AB_{3.8}$-type hydrogen storage alloy in alkaline electrolyte. *Russ. J. Electrochem.* **2015**, *51*, 244–248. [CrossRef]
147. Abe, H.; Aone, S.; Morimoto, R.; Uchida, H.; Ohshima, T. Improvement of hydrogen absorption characteristics of Pd using irradiation of heavy ions. *Trans. Mater. Res. Soc. Jpn.* **2011**, *36*, 133–135. [CrossRef]
148. Abe, H.; Tokuhira, S.; Uchida, H.; Ohshima, T. Surface modifications of hydrogen storage alloy by heavy ion beams with keV to MeV irradiation energies. *Nucl. Instrum. Methods Phys. Res. Sect. B Beam Interact. Mater. Atoms* **2015**, *365*, 214–217. [CrossRef]
149. Schulz, R.; Huot, J.; Liang, G.; Boily, S.; Lalande, G.; Denis, M.C.; Dodelet, J.P.; Banerjee, S. Recent developments in the applications of nanocrystalline materials to hydrogen technologies. *Mater. Sci. Eng. A* **1999**, *267*, 240–245. [CrossRef]
150. Zaluska, A.; Zaluski, L.; Ström-Olsen, J. Structure, catalysis and atomic reactions on the nano-scale: A systematic approach to metal hydrides for hydrogen storage. *Appl. Phys. A* **2001**, *72*, 157–165. [CrossRef]
151. Zhang, H.; Fu, L.; Xuan, W.; Qi, J. Surface modification of the $La_{1.7}Mg_{1.3}Ni_9$ alloy with trace Y_2O_3 related to the electrochemical hydrogen storage properties. *Renew. Energy* **2020**, *145*, 1572–1577. [CrossRef]
152. Uchida, H.H.; Watanabe, Y.; Matsumura, Y.; Uchida, H. Effect of KOH pretreatment on the hydriding properties of $LaNi_{2.5}C0_{2.5}$ alloy. *J. Alloy. Compd.* **1995**, *231*, 679–683. [CrossRef]
153. Wu, M.S.; Wu, H.R.; Wang, Y.Y.; Wan, C.C. Electrochemical investigation of hydrogen-storage alloy electrode with duplex surface modification. *Int. J. Hydrogen Energy* **2004**, *29*, 1263–1269. [CrossRef]
154. Kuriyama, N.; Sakai, T.; Miyamura, H.; Tanaka, H.; Uehara, I.; Meli, F.; Schlapbach, L. Surface treatment of a $LaNi_5$-type metal-hydride electrode with an alkaline solution dissolving cobalt (II) hydroxide. *J. Alloy. Compd.* **1996**, *238*, 128–140. [CrossRef]
155. Xiao, L.; Wang, Y.; Liu, Y.; Song, D.; Jiao, L.; Yuan, H. Influence of surface treatments on microstructure and electrochemical properties of $La_{0.7}Mg_{0.3}Ni_{2.4}Co_{0.6}$ hydrogen-storage alloy. *Int. J. Hydrogen Energy* **2008**, *33*, 3925–3929. [CrossRef]

156. Ramya, K.; Velayutham, G.; Subramaniam, C.K.; Rajalakshmi, N.; Dhathathreyan, K.S. Effect of solvents on the characteristics of Nafion®/PTFE composite membranes for fuel cell applications. *J. Power Sources* **2006**, *160*, 10–17. [CrossRef]
157. Patelli, N.; Migliori, A.; Morandi, V.; Pasquini, L. Interfaces within biphasic nanoparticles give a boost to magnesium-based hydrogen storage. *Nano Energy* **2020**, *72*, 104654. [CrossRef]
158. Wang, Y.; Wang, Y. Recent advances in additive-enhanced magnesium hydride for hydrogen storage. *Prog. Nat. Sci. Mater. Int.* **2017**, *27*, 41–49. [CrossRef]
159. Zhang, Y.; Wu, F.; Guemou, S.; Yu, H.; Zhang, L.; Wang, Y. Constructing Mg_2Co-Mg_2CoH_5 nano hydrogen pumps from $LiCoO_2$ nanosheets for boosting the hydrogen storage property of MgH_2. *Dalton Trans.* **2022**, *51*, 16195–16205. [CrossRef]

Disclaimer/Publisher's Note: The statements, opinions and data contained in all publications are solely those of the individual author(s) and contributor(s) and not of MDPI and/or the editor(s). MDPI and/or the editor(s) disclaim responsibility for any injury to people or property resulting from any ideas, methods, instructions or products referred to in the content.